BINOCULAR INFORMATION ACQUISITION AND VISUAL MEMORY

Thomas A. Busey
Indiana University

and

Geoffrey R. Loftus
University of Washington

Please send correspondence to:

Thomas A. Busey
Department of Psychology
Indiana University
Bloomington, IN 47405

email: busey@indiana.edu

Abstract

We investigate mechanisms underlying binocular combination of visual information within the context of a visual information acquisition theory proposed by G. Loftus, T. Busey, and their colleagues (e.g, as described by Busey & Loftus, 1994). A central assumption of the theory is that of a *sensory threshold*. By the theory, this threshold engenders an information loss in that information processing subsequent to the threshold is assumed to occur only when the magnitude of a *sensory representation* triggered by the stimulus exceeds the threshold. In this article, we describe research designed to investigate whether the presumed threshold is situated prior to or subsequent to the point at which the information from the two eyes combines. We also consider more general mechanisms of binocular combination and conclude that one must take the location of the sensory threshold into account when trying to interpret the nature of the binocular combination mechanisms. Evidence from three experiments provides strong conclusions both about the location of the sensory threshold(s) and about the mechanisms of binocular combination and binocular information acquisition.

Visual information acquisition begins with photons arriving at each of an observer's two eyes. The information contained in the pattern of arriving photons may represent something as simple as a monochromatic patch of light or as complicated as a naturalistic scene. Regardless of the stimulus, however, the geometry of binocular vision and the separation between the two eyes generally dictates that slightly different versions of this information arrive at each eye. Despite initially acquiring two separate representations of the visual scene, it is only under rare circumstances that observers report seeing more than one view of the world. This plus other evidence from the stereo depth perception literature (e.g. Julesz, 1971) and from the binocular combination literature (e.g., Blake & Fox, 1973; Blake, Sloane, & Fox, 1981) implies that the visual system must combine the outputs of the two eyes into a single unitary *sensory representation* and then based on this representation, proceed with further processing to acquire task-relevant information.

Loftus, Busey and their colleagues (Loftus, Busey & Senders, 1993; Loftus & Ruthruff, 1994; Busey & Loftus, 1994) proposed a theory of visual information acquisition consisting of a sensory front end followed by information acquisition components. The sensory front end is responsible for generating the sensory representation sketched above, and subsequent information acquisition mechanisms are responsible for acquiring task-relevant information. This theory successfully predicts performance in a number of different information processing paradigms, including digit recall (Loftus, Busey & Senders, 1993; Loftus, Duncan & Gehrig, 1992; Loftus & Ruthruff, 1994; Busey & Loftus, 1994); picture recognition (Loftus & McLean, in preparation); and synchrony judgment and partial report (Loftus & Irwin, under revision). Despite these successes, however, the current conceptualization of the theory does not specify how information from the two eyes combines to create a unitary sensory stimulus representation.

We have two goals in this article. Our first goal is to account for the mechanisms that combine information from the two eyes in information processing tasks. Our second goal is to examine the sources of information loss that result from a sensory non-linearity that proved essential to account for similar data. We will demonstrate that these two goals cannot be addressed separately, but are intimately related. Below we propose an extension of the Loftus and Busey theory, and focus on a crucial component of it termed a *sensory threshold*, which entails a specific source of information loss in the information processing pathway. We address two central questions: First, is the sensory threshold prior or subsequent to this point at which information from the two eyes combines? Second, what mechanisms are responsible for combining the two sources of information into a single unitary representation?

The range of binocular phenomenon is large, and we confine the domain of our theory building to relatively low-contrast stimuli. The vast majority of binocular summation experiments have been done with low-contrast stimuli presented for brief durations in detection tasks, and these findings

provide a good database from which combinatorial theories can be developed.

The major empirical question guiding binocular summation experiments has been: How much better are two eyes than one eye? The answer has not been simple. As detailed in excellent reviews by Blake and Fox (Blake & Fox, 1973; Blake, Slone & Fox, 1981), binocular performance may exceed monocular performance by various magnitudes. Binocular performance above monocular performance can be expected on statistical grounds, since a binocular stimulus provides two opportunities to detect a near-threshold stimulus. Blake and Fox (1973) formalized this into the Probability Summation prediction, with the assumption that the two observations were made independently. Other models of binocular combination can be produced through consideration of the neural mechanisms that combine the signals from two eyes, which include super-additive summation (interaction), additive (linear) summation, and sub-additive summation (inhibition). Interaction implies that the output of a system combining the inputs from the two eyes exceeds the sum of the inputs. Linear summation implies that the output is the sum of the inputs, and sub-additive summation implies that the output is less than the sum of the inputs. The probability summation prediction has become somewhat of a measuring stick from which conclusions about the combinatorial mechanisms can be derived. Blake and Fox (1973) conclude that if binocular performance exceeds a probability summation prediction based on monocular performance, this implies genuine neural interaction (that is, a super-additive summation mechanism). They argue that the probability summation model accordingly provides a baseline to detect greater-than-linear-summation combinatorial mechanisms.

Although the focus of the binocular combination experiments has been on the nature of the combination mechanisms (e.g. neural interaction, linear summation or inhibition), we will demonstrate that such questions cannot be addressed without consideration of both pre- and post-combinatorial sources of information loss. In particular, we will argue that a post-combinatorial threshold mechanism plays a major role when using binocular combination data to infer the mechanisms of combination.

The question of the combinatorial mechanisms subserving binocular combination is best addressed by varying the onsets of the presentations to each eye. For example, consider the probability summation model, that assumes that each eye provides an independent chance to detect a near-threshold stimulus. If this model holds, performance will remain constant if the two eyes are stimulated simultaneously, or if first one eye and then the other eye is stimulated. However, if binocular performance improves when the two presentations are made simultaneous, we would have evidence against the probability summation model. Thus the temporal overlap of the two presentation in a binocular condition provides a strong test of binocular summation models, and below we review relevant temporal overlap experiments.

Three important studies of binocular combination demonstrate the utility varying the temporal onset of the presentations to each eye of a binocular stimulus, and all three sets of authors have argued for neural interactions (above-linear summation) between the two eyes to produce binocular performance. Westendorf, Blake & Fox (1972) presented contrast increments to both eyes in a detection task. The stimulus onset asynchrony (SOA) between the two presentations was either 0 ms or 100 ms. They found binocular performance above a probability summation prediction for the simultaneous presentations, but binocular performance consistent with probability summation for the 100 ms SOA. They concluded that binocular performance cannot be predicted solely from probabilistic considerations, and instead the superiority at 0 ms SOA resulted from neural interaction between the two eyes.

An earlier study by Matin (1962) demonstrated the utility of varying the temporal overlap of the two presentations. He varied the interval separating the two flashes of a binocular presentation over a wide range, and found that SOAs less than 100 ms produced binocular performance that is superior to the probability summation prediction. He concluded that the two eyes were not independent detectors, but detection instead resulted from neural summation between the two eyes.

Although much of the work on binocular summation has relied on detection tasks, Eriksen and his colleagues (Eriksen, Greenspon, Lappin & Carlson, 1966; Eriksen & Greenspon, 1968) examined letter identification in a three-alternative forced-choice procedure. As with previous findings, he found that for SOA's shorter than 50 ms, binocular performance exceeds the probability summation prediction.

The overwhelming evidence disconfirms a probability summation mechanism, and has lead many authors to posit neural interaction as the combination mechanism mediating binocular combination. However, these data also clearly indicate that no single combinatorial mechanism can account for binocular summation at all SOA's, since binocular performance changes with SOA. Thus a complete description must account for the amount of temporal overlap that is produced by a non-zero SOA binocular stimulus. The present article represents such an approach, although it is motivated, in part, by extant binocular summation models. Two of the most influential are the binocular energy detector model of Legge (1984a, 1984b) and the interocular suppression model of Cogan (1987, 1991).

The binocular energy detector model extends the signal detection model of Green and Swets (1966, 1974) to binocular summation. The model consists of two monocular channels that are subjected to input noise before undergoing a squaring function. The results are linearly summed and the final binocular output results from a compressive nonlinearity and the addition of central noise. This model predicts a quadratic summation relationship between binocular and monocular thresholds, which results from the fact that when two noisy signals are added, the standard deviation

increases by the square root of the number of signals. While this model can account for a diverse range of low-contrast phenomenon, the lack of temporal coding of the stimuli leaves the model unable to account for non-zero SOA binocular presentations.

Alexander Cogan (Cogan, 1987; 1991) presents a model that can qualitatively account for the effects of varying the SOA between the two presentations of a binocular stimulus. We describe this model and fit it to our data in the General Discussion section; briefly it is as follows. The combination mechanism chosen by Cogan is relatively complex: information registering in either eye both provides excitatory input to the monocular channel and inhibits the other monocular channel. In a separate mechanism, the information from the two eyes combines into a binocular fused channel, and the final binocular output is the sum of the combined monocular channels and the binocular fused channel. This model accounts for increments and decrements in binocular and monocular presentations and will also qualitatively account for the effects of non-zero SOA's in binocular presentations. However, Cogan does not provide quantitative fits to the variable-SOA data. The importance of quantitative fits will become apparent in the discussion section of the current article, but to anticipate, two models that share similar theoretical structures and thus provide qualitatively identical predictions do not give the same quantitative predictions. Indeed, we will test and disconfirm Cogan's model based on poor quantitative fits.

One conclusion is clear from the existing binocular summation data and theories: A complete account of binocular summation must include both descriptions of how information from two eyes combines, as well as how this relationship changes as the SOA between the two presentations is varied. This, along with a description of the sources of information loss that contribute to performance, is the major theoretical contribution of the current work.

The remainder of this article is organized as follows. First, we explicitly describe the task that we are trying to model. Second, we briefly outline the Busey/Loftus theory, and propose two (not mutually exclusive) candidate extensions to it that may account for performance in tasks designed expressly to investigate binocular combination. Third, we describe data from three experiments designed to evaluate the two extensions and, more generally, to reveal the nature of the information combination mechanisms. Fourth, we conclude that neither extension alone will completely account for all of the observed characteristics of the data, although a combination of the two does provide a good account of the data. Fifth, we make specific conclusions about the nature of the information combination mechanisms and, based on these conclusions, describe theoretical implications for researchers studying the nature of the combinatorial mechanisms. Finally, we apply Cogan's model to our data to examine how the choice of combination mechanisms affects our conclusions. We will argue that the question of the nature of the combinatorial mechanism is intimately tied to the question of the location of the sensory threshold and that above-probability summation binocular

performance need not imply neural interactions between the to monocular channels.

An Information Processing Task

The task that we will attempt to model is complex enough to provide generalizability to everyday tasks, but simple enough to be plausibly described with a relatively simple and concise theory. In this task, four digits are presented to an observer whose job is to report as many of them as possible, in their correct order, guessing if necessary. The basic performance measure, p, is the proportion of correctly-reported digits, in their correct locations, adjusted for the guessing probability of 0.10[1].

THEORY

Busey & Loftus (1994) have described a theory that has successfully accounted for performance in this digit-recall task[2]. In this section we summarize the theory, while in the next section, we develop two extensions of it designed to account for the combinatorial mechanisms involved in binocularly viewed stimuli. This theory conjoins a linear-filter front end, common in the vision literature, with an independent sampling model that operates on the output of the linear-filter front end to acquire task-relevant information.

Linear-Filter Front End

The initial response in the visual system to a briefly-presented stimulus can be modeled as the output of a band-pass or low-pass *linear filter* (e.g. Sperling and Melchner, 1968; Watson, 1984). Rapid temporal changes in the stimulus are temporally blurred by a visual system that cannot keep up with the stimulus; slower temporal changes are better represented. The exact nature of the response can be derived by assuming an *impulse-response function* for the linear filter that describes the severity of the temporal blurring, or, thought of in another way the amount of response that persists following the termination of the physical stimulus. Under low-luminance conditions such as the ones used in our experiments, the filter is usually assumed to be low-pass, meaning that the visual system reproduces progressively higher temporal frequencies progressively less faithfully.

The shape of the impulse response function, g(t), dictates the type of temporal blurring. In keeping with previous sensory literature (e.g. Watson, 1979, 1986) I have chosen this function to be the difference of a two gamma functions, each with a different time constant,

---

[1]The guessing formula is p = (x - 0.1)/0.9 where x is the raw proportion correct and p is the corrected proportion.

[2]See also, Loftus, Busey, & Senders (1993) and Loftus & Ruthruff (1994).

$$g(t) = \frac{(t/\tau)^{n-1}e^{-t/\tau}}{\tau(n-1)!} - s\left[\frac{(t/r\tau)^{n-1}e^{-t/r\tau}}{r\tau(n-1)!}\right] \quad \text{Eq. 1}$$

where τ represents the time-constant of the gamma function and provides an estimate of the temporal response properties of the mechanisms mediating a given task. The sensory response function component of the LST theory (a(t)) is based on work from Andrew Watson (Watson, 1986), George Sperling (Sperling and Sondhi, 1968) and others working in the temporal domain of perception. Figure 1, left panel, shows example impulse response functions.

The first term in Eq. 1 represents an excitatory component, while the second term represents an inhibitory component of the response, which tends to sharpen the response and allows it to respond to higher temporal frequencies. The parameter *r* represents the ratio of the time-constant of the inhibitory component of the response to the excitatory component of the response, and *s* represents the magnitude of the temporal inhibition component. The parameter n represents the number of stages in each process, and for the current modeling we fix it at 9, although the shape of the impulse-response function is relatively unchanged by the precise value chosen.

Identification data for letter stimuli such as those used in the present study are often modeled by setting *s* to 0 (Busey, 1994), which gives a *monotonic* impulse response function g(t) as shown as a solid curve in the left panel of Figure 1. An alternative way of representing the same information is by taking the Fourier transform of the impulse response function g(t), which results in a temporal contrast sensitivity function (TCSF). The TCSF plot show the sensitivity of a system to different temporal frequencies. The TCSF corresponding to the solid line in the left panel of Figure 1 is given by the solid line in the right panel. These curves represent a purely sustained response, and give a monotonically-decreasing TCSF, as shown in Figure 1, right panel.

INSERT FIGURE 1 ABOUT HERE

Detection data for stimuli containing mainly low spatial frequencies, or stimuli presented on bright backgrounds, often are modeled by $s > 0$. In this case the impulse response inhibits processing after an initial excitatory response, which results in an inhibitory lobe in the impulse response function g(t) (dashed line in Figure 1, left panel) and a characteristic TCSF with a decrease in sensitivity at low temporal frequencies (dashed curve in Figure 1, right panel).

The temporal characteristics of the physical stimulus are summarized by a function describing contrast over time since stimulus onset, called the *stimulus input function*. For the stimuli discussed here, the digits simply appeared at some contrast, Φ, for the appropriate stimulus duration, and then disappeared. Thus the stimulus input function f(t) can be described as:

$$f(t) = \begin{cases} \Phi & (0 \le t \le d) \\ 0 & \text{elsewhere} \end{cases} \qquad \text{Eq. 2}$$

where Φ represents stimulus contrast and t is time since stimulus onset[3].

We term the visual system's response to such a stimulus a *sensory response function*, denoted a(t), which is computed by convolving the stimulus input function with the impulse response function:

$$a(t) = f(t) * g(t) \qquad \text{Eq. 3}$$

where "$*$" represents convolution. The sensory response function represents the output of the linear-filter stage of the theory, and describes the initial representation of a visual stimulus.

Further information acquisition mechanisms act on this representation to acquire task-relevant information. However, prior to becoming available for information acquisition, the sensory response function is assumed to pass through a threshold device, such that only the portion of the sensory response function that exceeds a *sensory threshold* is available for information acquisition. Thus we define a new function $a_\Theta(t)$:

$$a_\Theta(t) = \begin{cases} a(t) - \Theta & (a(t) > \Theta) \\ 0 & (a(t) \le \Theta) \end{cases} \qquad \text{Eq. 4}$$

where Θ is the magnitude of the sensory threshold. Information acquisition cannot begin until a(t) exceeds the sensory threshold. As described below, once the information acquisition process begins it proceeds at a rate that is proportional to $a_\Theta(t)$. Before turning to this issue, however, some notes on the nature of the sensory non-linearity are in order. The behavior of the sensory threshold described in Eq. 4 can be mimicked by other non-linearities, and in particular by a power function of the form:

$$a_\beta(t) = [a_p(t)]^\beta$$

This power function has be used by Watson (1972) in his probability summation in time model and by Legge (1984a, b) in a binocular summation model with $\beta = 2$. We have chosen to fit models with both non-linearities, and in general we find the two formulations equivalent. However, the threshold model gives slightly better fits to the data and is also slightly easier to demonstrate graphically. In addition, there is neurological evidence in favor of this formulation from Ohzawa &

---

[3]Because the stimuli were displayed on a computer monitor, the actual function f(t) flickered at 75 Hz, albeit at a rate faster than typically resolvable by the human eye. However, given Appendix C of Busey & Loftus (1994) this has little implication for our theory.

Freeman (1986), as discussed in the General Discussion. For these reasons, as well as for consistency with previous formulations (Busey & Loftus, 1994), we present the model predictions in terms of the threshold model.

Acquired Information: The Information-Acquisition Rate

Once the sensory response function exceeds the sensory threshold, information acquisition can begin. At time t following stimulus onset information acquisition proceeds at an instantaneous rate, termed the *information acquisition rate*, denoted r(t), which is proportional to the product of (1) the magnitude of above-threshold sensory response and (2) some decreasing function of already-acquired information. The particular form of the information acquisition formulation is similar to independent sampling models proposed by Townsend (1981), Shibuya & Bundesen (1988), Rumelhart (1970), and Massaro (1970); viz., information is presumed to be acquired at random and with replacement. The independent-sampling assumption implies that the *rate* of acquiring information is constant, and governed by a scaling parameter $1/c_s$. However, because information is sampled from the stimulus with replacement, the rate of acquiring *new* information is proportional to the amount of not-yet-acquired information.

More specifically, let I(t) be the proportion of acquired information at time t. The *information acquisition rate*, r(t), is by definition the derivative of I(t) with respect to time, and is given by:

$$r(t) \equiv \frac{dI}{dt} = a_{\Theta}(t)\left[\frac{1.0 - I(t)}{c_s}\right] \qquad \text{Eq. 5}$$

Eq. 5 states that the rate of acquiring new stimulus information is proportional to the product of the above-threshold sensory response and the remaining stimulus information, with a constant of proportionality $1/c_s$.

It is simple to show (e.g., Busey & Loftus 1994) that with this rate function, the function relating total acquired information, denoted I(∞), to the above-threshold area under $a_{\Theta}(t)$, denoted $A_{\Theta}(\infty)$, is given by,

$$I(\infty) = 1.0 - e^{-A_{\Theta}(\infty)/c_s} \qquad \text{Eq. 6}$$

One additional linking hypothesis is required to make quantitative predictions, which is that p, the proportion of correctly-recalled digits, equals the total proportion of acquired information I(∞). Given this and Eq. 6,

$$p = 1.0 - e^{-A_{\Theta}(\infty)/c_s} \qquad \text{Eq. 7}$$

An important consequence of Equation 7 is that performance, p, is monotonically related to the above-threshold area under the sensory-response function. This implies that if condition i results in

more above-threshold area, $A_{\Theta}(\infty)$ than condition j, the theory predicts that performance from condition i will exceed that from condition j. In addition, any two conditions that produce the same above-threshold area $A_{\Theta}(\infty)$, are predicted to have the same performance. Although Equation 7 provides a stronger description of the area/performance relation than monotonicity, for purposes of exposition it is convenient to think in terms of the consequences of the monotonicity relation, which is that *more above-threshold-area implies greater performance*.

At the risk of redundancy, we emphasize that these relations are a *consequence* of Eqs. 1, 3, 4, 5 and 6 and are *not* assumptions of the theory. It is also worthwhile to note that the prediction of Eq. 7 is also independent of the choice of stimulus wave form, not just the rectangular wave form given in Eq. 2.

Testing Eq. 7 requires an experimental design that varies $A_{\Theta}(\infty)$, the above-threshold area under the sensory response function. We typically vary the stimulus duration of several different types of conditions, including binocular, monocular and dichoptic stimuli, in order to produce empirical data that provides a strong test of the theory. When plotted against stimulus duration, digit-recall performance in a given condition is called a *performance curve.*

Figure 2 demonstrates the different model components and their relations.

INSERT FIGURE 2 ABOUT HERE

The above model formulations do not explicitly assume the presence of noise, although, as discussed below, the sensory threshold may be thought of as representing the amount of signal lost to noise. The binocular energy model of Legge (1984a, b) assumes both input and central sources of noise, although formulations by Cogan (1987) do no explicitly assume noise. Noise could be explicitly incorporated into the model without changing the formulations by assuming that the height of the sensory response function gives the probability that the signal exceeds the noise at that particular instance. This is the interpretation adopted by Watson's probability summation in time (Watson, 1979), and this makes the power-function formulation of the model similar to Legge's (1984a, b) model.

Note that complete equations for all model formulations are given in Appendix A.

THE ROLE OF THE SENSORY THRESHOLD IN BINOCULAR COMBINATION OF OCULAR CHANNELS

The sensory threshold described in the previous section is assumed to exist prior to the information acquisition components of the information processing pathway. As a result, we consider it a sensory component. Because no further information processing takes place unless the sensory response exceeds threshold, the threshold can be considered a source of information loss. We now ask: Does this information loss occur before or after the information from each eye is

combined into a central unitary representation?

Below we describe two models that address this question. Each model extends the previously-described theory by assuming that information enters each eye and engenders in each eye an initial *peripheral* sensory response function. These two peripheral sensory response functions then combine centrally to provide a single *central* sensory response function. Information is acquired based on this central sensory response function and further processing, or a task-relevant response, is made based on the amount of acquired information. We describe these two models within the context of Experiment 1, which is designed to evaluate them.

Experiment 1: Is the a(t) Threshold Prior or Subsequent to Binocular Combination?

In Experiment 1 we used monocular, binocular, and dichoptic stimuli. A monocular stimulus is presented to one eye only. A binocular stimulus is presented to both eyes simultaneously. A dichoptic stimulus consists of two temporal stimulus halves, presented successively, with zero ISI: the stimulus is presented first to one eye and then immediately to the other eye.

As we shall see, comparison of performance curves for these three presentation types will allow us to isolate the location of the presumed sensory threshold. To do so, we must extend our theory such that it takes these three presentation types into account. We first assume that information from each eye is carried by a *monocular channel,* and that each monocular channel generates a *peripheral a(t) curve*. The information from the monocular channels combines to produce a *central a(t) curve,* upon which memory performance is based. As an extension of linearity, we further assume that the two peripheral a(t) curves *sum* to produce the central a(t) curve[4].

Support for our assumption of a linear combination mechanism comes from single-cell recording done with simple cells in cat by Ohzawa and Freeman (1986). Using sine-wave gratings tuned to the cell's optimal orientation, they found that the light-evoked neural responses from each eye are summed linearly to produce the output of a binocular cell. Interestingly, they also found a minority of cells that deviate from this linearity prediction, which they attribute to a threshold mechanism that occurs after the linear binocular summation. We will return to this in our Discussion section.

The linearity assumption also allows quantitative evaluation of the sources of information loss, both before and after the site of binocular combination. Such a summation mechanism was adopted

[4]An alternative formulation has been suggested by Randolph Blake (personal communication). Rather than two independent monocular channels, Blake suggests thinking in terms of binocularly-tuned neurons that vary in their ocular dominance. Either formulation allows consideration of the question "is the information loss (due to the a(t) threshold) pre- or post-binocular combination?"

by Legge, although his additional assumptions about noise may provide for different predictions of binocular performance. A more complex combination mechanism developed by Cogan (1987) is discussed in a subsequent section.

Given the assumptions described above, we are able to ask: is there an a(t) threshold for the peripheral a(t) functions, for the central a(t) curves, or for both?

Two Models

Figure 3 illustrates these two possibilities. To illustrate them, we show the responses generated by an 80-ms dichoptic presentation (which, of course, involves a 40-ms presentation to one eye followed by a 40-ms presentation to the other eye) are shown. The top half of Figure 3 shows the *peripheral a(t) threshold model*, by which a peripheral threshold, Θ_p, is assumed on the a(t) functions generated by each monocular channel. Only the above-peripheral-threshold area from the peripheral a(t) curves combines to form the central a(t) curve. All of the central a(t) curve area contributes to performance.

INSERT FIGURE 3 ABOUT HERE

The bottom half of Figure 3 shows the *central a(t) threshold model*, by which a central threshold, Θ_c, is assumed on the central a(t) curve. All of the peripheral-curve area contributes to the central a(t) curve, but only the above-central-threshold area contributes to performance.

Note that all model equations appear in Appendix A.

Predictions: Monocular vs. Dichoptic Conditions

Evaluating these two candidate models entails the following logic. Consider an 80 ms *monocular* presentation and its corresponding a(t) curve, shown in the left panel of Figure 4. This monocular presentation implies the same above-central-threshold area (1.4 in this example) for both peripheral and central a(t) threshold models. The location of a sensory threshold is irrelevant for this condition because information is presented to only one eye, and there is no information to combine from the other eye. This makes the monocular condition a good comparison stimulus because monocular performance is predicted to be the same by both models.

INSERT FIGURE 4 ABOUT HERE

Now consider a *dichoptic* presentation in which the 80-ms duration is broken into two 40 ms presentations, the first to one eye, and the second to the other eye *with a zero ISI*[5]. The peripheral

[5]Because the stimuli were displayed on a computer monitor, the actual ISI was equal to the monitor's refresh rate, or 15 ms. However, the monocular and dichoptic displays all had the same presentation time course, e.g. 6 refreshes to one eye, verses 3 refreshes to one eye followed by 3 refreshes to the other eye. Given this, we can safely assert that the effective ISI was zero, a presumption we will make throughout the rest of this article. Appendix C of Busey & Loftus (1994) discusses this issue in detail.

and central a(t) threshold models yield different predictions for this condition. The middle panel of Figure 4 shows the central a(t) curve prediction for the peripheral-threshold model. Only the above-peripheral-threshold area contributes to the central a(t) curve, but all of the central-a(t)-curve area contributes to performance. Because the area reaching the central a(t) curve is smaller than the above-threshold area in the monocular condition, *the peripheral-threshold model predicts dichoptic performance to be lower than monocular performance*. As we will show next, a finding of poorer dichoptic relative to monocular performance is not only consistent with a peripheral-threshold model, but also *disconfirms* any model in which the sole threshold is central.

The right panel of Figure 4 shows the central a(t) curve for a dichoptic presentation predicted from the central a(t) threshold model. The dashed curves are the peripheral a(t) curves before they combine to produce the central a(t) curve. Because the two peripheral a(t) curves combine before the central a(t) threshold, the dichoptic central a(t) curve is identical to the monocular central a(t) curve, and they have the same above-central-threshold area. Thus *the central-threshold model predicts monocular and dichoptic performance to be identical*. It is for this reason that a finding of poorer dichoptic compared to monocular performance disconfirms a purely central-threshold model.

Predictions: Monocular vs. Binocular Conditions

A second set of predictions involves comparison of the monocular and binocular conditions. In general the means by which information from two eyes is combined to produce binocular information—and, correspondingly, the relation between performance based on a monocular versus a binocular presentation—is the source of some debate (Legge, 1984b; Blake & Fox, 1973; Blake, Sloane & Fox, 1981). Two reasonable propositions have been put forth: first that the combination occurs via probability summation, and second that the combination occurs via quadratic summation. In our General Discussion we evaluate a third proposition that assumes neural interaction between the two ocular channels in a binocular presentation.

The supposition that the information combines via probability summation is easily incorporated by our theory. In the section below we develop a version of the theory that gives a prediction consistent with probability summation, and to do so we begin with probability summation and work backwards. Consider any two information sources (e.g., first and second presentations; left eye and right eye; etc.) and denote the proportions correct based on these two sources as p_1 and p_2. If p_B denotes proportion correct given both information sources, then probability summation implies that,

$$p_B = p_L + (1.0 - p_L)p_R \qquad \text{Eq. 8}$$

or,

$$(1.0 - p_B) = (1.0 - p_L)(1.0 - p_R) \qquad \text{Eq. 9}$$

Substituting $1.0 - e^{-A_\Theta(\infty)/c_s}$ (Eq. 7) for each p and simplifying we find:

$$e^{-A_{\Theta,B}(\infty)/c_s} = (e^{-A_{\Theta,L}(\infty)/c_s})(e^{-A_{\Theta,R}(\infty)/c_s})$$

and taking the natural log of each side of the equation,

$$A_{\Theta,B}(\infty) = A_{\Theta,L}(\infty) + A_{\Theta,R}(\infty) \qquad \text{Eq. 10}$$

Thus Equation 10 may be interpreted to mean that two separate areas (e.g., two areas corresponding to performance from the two eyes separately) *sum* to produce a total area corresponding to performance in the combined (e.g., binocular) condition. Thus probability summation entails simply summing the two peripheral a(t) curves over t to generate the central a(t) curve. Assuming equal contributions from both eyes, i.e. $A_{\Theta,L}(\infty) = A_{\Theta,R}(\infty) = A_{\Theta,M}(\infty)$, then $A_{\Theta,B}(\infty) = 2A_{\Theta,M}(\infty)$ and

$$p_B = 2p_M - p_M^2 \qquad \text{Eq. 11}$$

where p_B and p_M correspond to binocular and monocular performance respectively. Note that this assumes that the sensory threshold Θ is assessed *before* the site of combination, and that the information-processing rates c_s are the same for both eyes. Thus we are considering the peripheral threshold model for the moment.

We began this section by using the probability summation equation (Eq. 9), and worked backwards to produce a version of the theory that is consistent with Eq. 9. The goal was to detail those assumptions necessary to produce the probability summation prediction. To summarize, if, in addition to the assumptions embodied in Eqs. 4, 5 and 6, we also assume a linear combination mechanism and no post-combination information loss, then the theory will make a prediction that is consistent with probability summation (Eq. 11). This is because the above-threshold area engendered by a binocular presentation is twice that engendered by a monocular presentation under a peripheral threshold model.

Note that the probability summation prediction is a *consequence* of the assumptions of a linear summation mechanism and no post-combinatorial information loss. Other models have adopted a linear summation mechanism and other assumptions and derive a different prediction of binocular performance based on monocular data.

Linear summation does not imply a probability summation prediction

At this point we wish to clearly distinguish between a probability summation prediction, which is a prediction of binocular performance based on monocular data, and a theory that assumes a *linear-summation* combination mechanism. The latter is a model of how the information from two eyes combines. When a linear-summation mechanism is conjoined with additional assumptions of

no post-combinatorial information loss and an independent sampling information-acquisition mechanism, then a linear-summation mechanisms will make a prediction that is consistent with probability summation. *However, as we will show below, a theory that assumes a linear-summation combination mechanism will make predictions that differ from probability summation if a different set of assumptions about thresholds are made.* Thus the question of combination mechanisms is intimately tied to the question of threshold locations; one cannot simply compare monocular and binocular data and infer the combinatorial mechanisms without also considering pre- and post-combination information losses. This is a major theme of the current work. We shall refer to a model that sums the information from two eyes as a linear-summation combination mechanism, which under certain assumptions will predict probability summation, but which under other assumptions will not.

When we refer to predictions of binocular data based on monocular performance, we shall call this a *probability summation* prediction. When we refer to a specific model of binocular information combination that explicitly assumes a linear summation combination mechanisms and may, under certain assumptions, make a prediction of binocular performance that is consistent with probability summation, we shall refer to this as a *linear-summation* model.

We are now in a position to discuss the model's predictions about the relation between the monocular and the binocular conditions. First consider the predictions for a peripheral threshold model, as shown in the top panel of Figure 5. In a monocular presentation, the digits appear in only one eye and generate only a single peripheral a(t) curve. The area that survives the peripheral threshold constitutes the central a(t) curve.

INSERT FIGURE 5 ABOUT HERE

In a binocular presentation, the digits are presented to both eyes, and generate two peripheral a(t) curves. These two curves will both pass through peripheral a(t) thresholds, and because the contrast of the two presentations is always the same, the two peripheral curves will be identical[6]. As a result, the binocular conditions central a(t) curve will always be twice as high as the monocular condition's central a(t) curve, and thus the binocular area will always be twice as great. This implies that *under a peripheral threshold model binocular performance will fulfill a probability*

[6]The statement that both eyes contribute identical responses is a simplification, given that most observers have a dominant eye. However, any performance asymmetry between the two will simply bring binocular performance closer to the averaged monocular performance. Consider the extreme case where an observer is blind in one eye. In this case binocular performance will be exactly double the across-eye averaged monocular performance: binocular performance will equal performance from the sighted eye, which is then averaged with zero performance from the blind eye. Our argument for the existence of a central threshold requires that binocular performance be *greater* than twice the monocular performance. However any asymmetry serves to reduce the difference between monocular and binocular performance, and cannot *increase* the difference between binocular and averaged-monocular performance.

summation relation with monocular performance: $p_B = 2p_M - p_M^2$. (see the top panel of Figure 5). Note that this is in accordance with the probability summation prediction of Eq. 11, although we have now described a specific model that makes a probability summation prediction. This model makes two key assumptions: no post-combinatorial source of information loss and a linear-summation combinatorial mechanism.

By the central-threshold model, however, binocular performance is predicted to be *greater* than is predicted by probability summation. The logic underlying this assertion is illustrated in the bottom panel of Figure 5. In the absence of peripheral thresholds, the two curves are the original monocular and binocular a(t) curves. As in the top panel the binocular curve is *overall* twice as tall as the monocular curve. However, there is now a central a(t) threshold, and only the above-central-threshold area determines performance.

Note that much of the monocular area falls below the central threshold, leaving only an area of 1.4 above threshold in this example. In contrast the binocular curve, by virtue of being higher than its monocular counterpart, is relatively less affected by the same threshold; hence the binocular *above-threshold* area (4.1 in this example) is greater than twice the monocular above-threshold area (of 1.4). This implies binocular performance *above* the probability-summation prediction (i.e. $p_B > 2p_M - p_M^2$). This above-probability-summation prediction holds for any non-zero central a(t) threshold (except for the trivial case when neither curve exceeds threshold and performance is zero in both conditions). This above-probability summation prediction is a direct result of the central a(t) threshold.

Prediction Summary

Let us summarize two critical predictions for Experiment 1. First, a finding that monocular performance exceeds dichoptic performance disconfirms a purely central-threshold model, and confirms a peripheral-threshold model. Second, a finding that binocular performance exceeds what would be predicted on the basis of probability summation from the monocular condition disconfirms a purely peripheral model and confirms a central-threshold model.

Method

There were three main conditions in Experiment 1. In the first (monocular) condition a single d-ms stimulus was displayed to only one eye. In the second (dichoptic) condition there were two stimulus presentations, each d/2 ms in duration, separated by a zero-ms ISI. The first d/2 ms was displayed to one eye, while the second d/2 ms was displayed to the opposite eye. In the third (binocular) condition a d-ms stimulus was presented to both eyes simultaneously.

Observers

Three experienced vision researchers participated in Experiment 1. Observer TB is the first

author. Observers GW and TAK were visiting faculty members.

Stimuli and Apparatus

Stimulus presentation (and response collection) in Experiments 1-3 were carried out on a Macintosh II computer. Stimuli were displayed on an Apple Monochrome monitor in conjunction with a Modified Wheatstone mirror stereoscope (see Blake & Fox, 1973). The refresh rate (67 Hz) of the display device was sufficiently fast to eliminate flicker, and poses little interpretational problem for our theory (See Busey & Loftus, 1994, Appendix C).

Subjects sat approximately 57 cm away from the screen in a dimly lit room, and used the computer keypad to respond. A chin rest positioned the observer's head in front of two mirror arrangements that projected each half of the screen to one of the observer's eyes. An enclosing box eliminated reflections from the screen and assisted with eye fusion.

Considerable effort was taken at the start of each block of trials to fuse the two halves of the monitor into one image without eye strain. Observers adjusted each of the four mirrors until the fixation point fused into a single image. They then adjusted the mirrors to create a cross out of two right angles, each of which was shown only to one eye. Figure 6 shows the experimental apparatus and the image used to adjust the mirrors. To further enhance eye fusion within a session, the background was a uniform gray field, and the fixation point never disappeared.

INSERT FIGURE 6 ABOUT HERE

The digits were presented in 24 point Times-Roman font. The digits were each 0.50° high by 0.40° wide, separated by 0.75° vertically and 0.40° horizontally. Table 1 lists the luminances and contrasts. Darker letters on a lighter background were used to avoid phosphor-decay problems. The experiment was programmed using a timing and display package described by Ames & Palmer (1992).

INSERT TABLE 1 ABOUT HERE

Design and Procedure

There were 8 monocular and dichoptic stimulus durations, ranging from 30 - 240 ms in 30-ms increments. In the monocular condition the entire d-ms duration was shown to either the right or left eye. In a corresponding dichoptic condition, d/2 ms of a d-ms presentation was shown to either the right or left eye, followed immediately by the second (d/2)-ms presentation to the *opposite* eye, with zero ms ISI. Eye position was randomized across all conditions. In the binocular condition, there were 7 durations, ranging from 30 ms to 119 ms in 15-ms increments. During monocular and dichoptic presentations, the eye opposite the stimulated eye saw the blank background field.

Observers completed 18, 72-trial blocks, which provided 54 replications of each conditions per

observer[7].

Results

Figure 7 shows the data for Experiment 1, along with the predictions from the peripheral threshold model. Details of the parameter fitting procedures and equations are found in Appendix A. No notable performance differences exist for the three observers, and thus the data shown are averaged across observers. The upper (binocular) solid line represents the model's prediction of binocular performance based on probability summation from the monocular condition. In this, as in all data figures, error bars represent standard errors, and the "RMSE" at the lower right is the root-mean-square error between the data points and the predicted values.

INSERT FIGURE 7 ABOUT HERE

Two findings and associated conclusions are apparent. First, the finding that dichoptic performance is below monocular performance allows us to reject a pure *central-threshold model*. Second, the finding that binocular performance is above the probability summation prediction allows us to reject a pure *peripheral threshold model*.

Discussion

The failure of both single-threshold models to account for performance in all three conditions leaves open the possibility that there is *both* a peripheral and a central threshold. Let us summarize the logic underlying this assertion.

The observed binocular performance above that predicted from probability summation indicates that a complete model requires a central threshold. This central threshold hinders monocular performance more than binocular performance, because the two monocular channels of a binocular presentation combine *before* the central threshold is assessed. The above-threshold binocular a(t) curve is therefore more than twice as high as an equal-duration monocular curve.

The observed inferiority of dichoptic relative to monocular performance indicates that a complete model must also include a peripheral threshold. The performance decrement for dichoptic presentations relative to monocular performance implies some form of information loss *prior* to the combination of the two ocular channels; such loss occurs with a peripheral threshold.

To summarize, we have rejected the pure forms of the peripheral and central a(t) threshold models, and concluded that *both* the peripheral and central a(t) thresholds are necessary. We now

---

[7]The experimental design for Experiment 1 originally called for 8 durations for each of the three conditions. However, during tachistosopic verification of the stimuli, the 15 ms binocular condition actually resulted in a 30 ms presentation. Therefore the data for this condition was averaged with the 30 ms condition, giving 108 replications of the 30 ms binocular condition.

alter our theory to account for these findings. Essentially, we do this by dividing the formerly single a(t) threshold into peripheral and central a(t) thresholds.

The Dual-Threshold Model

Figure 8 illustrates this modified model, which we call the dual-threshold model. Each ocular channel produces an a(t) function, complete with peripheral threshold. The above-threshold areas from each channel sum to produce the central a(t) function, which includes a central threshold. Performance is related to the above-central threshold area, $A_{\Theta_c}(\infty)$, by Eq. 7.

INSERT FIGURE 8 ABOUT HERE

$$a_c(t) = a_{\theta,L}(t) + a_{\theta,R}(t)$$

$$a_{\Theta,c}(t) = \begin{cases} a_c(t) - \Theta_c & (a_c(t) > \Theta_c) \\ 0 & (a_c(t) \le \Theta_c) \end{cases} \quad \text{Eq. 12}$$

Figure 9 shows the modified theory's best fit to the Experiment 1 data. The fit is extremely close, with a RMSE of 0.0189. Table 2 lists the parameter values for each observer and for the fit in Figure 9. Note that the assumption of a central threshold implies a model that contains a linear-summation mechanism but no longer makes a probability summation prediction of $p_B = 2p_M - p_M^2$.

INSERT FIGURE 9 ABOUT HERE

Note that the site of information loss is relative to the combinatorial mechanisms. Information lost during the combination process, such as sub-additive summation, would be considered post-combinatorial information loss because it would affect both the left- and right-eye information. Pre-combinatorial information losses affect only the information from a single eye.

INSERT TABLE 2 ABOUT HERE

Accounting for Previous Data

Given the necessity of two thresholds to adequately describe the Experiment 1 data, we might ask how previous experiments using similar stimuli, such as those described in Busey and Loftus (1994), could be fit by a single-threshold model. The answer is that, mathematically, the previously assumed single threshold subsumes both thresholds. The two thresholds simply combined and were represented by a single threshold. Only when the binocular and dichoptic conditions were included did the two thresholds reveal themselves. The dual-threshold model would, of course, also fit the data from Experiments 1-6 of Busey & Loftus (1994), albeit with 100% tradeoff between the two threshold parameters.

Dual-Threshold Model Predictions for Dichoptic and Gap-Monocular Presentations

A further test of the dual-threshold model comes from comparing three conditions. Experiment 4 of Busey and Loftus (1994) included the present monocular condition, as well as a related condition called a *gap-monocular* condition, in which the total duration (d) of the monocular presentation was split into two temporal (d/2)-ms halves, separated by a 250-ms blank screen. Observers performed substantially better in the monocular compared to the gap-monocular condition. As Busey and Loftus showed, this is predicted by the theory, which implies more a(t) area above threshold in the monocular than in the gap-monocular condition.

The dichoptic condition of Experiment 1 is analogous to a gap-monocular condition, except for the zero ms ISI and the presentation of each pulse to different eyes. Dichoptic condition performance is, like gap-monocular condition performance, worse than monocular performance. This is implied by the theory in part because a dichoptic condition suffers the effects of two peripheral thresholds, while a monocular presentation suffers from only a single peripheral threshold.

The dichoptic and gap-monocular conditions are related in that in both, the stimulus is divided into two temporal halves, and performance in both conditions is worse than monocular performance. However, the dual-threshold model predicts a performance difference between these two conditions. The reason will be described in detail below, but briefly it is this. The dichoptic condition's zero ISI allows the two peripheral a(t) curves to overlap and sum, and thus provides more above-central-threshold area under the central a(t) curve compared to a gap-monocular condition. The gap-monocular condition's large ISI prevents the two peripheral a(t) curves from interacting, leaving less above-central-threshold area. Thus, on the basis of the slightly more area above the dichoptic curve's central a(t) threshold, the dual-threshold version of the theory predicts a slight performance advantage for the dichoptic condition, compared to the gap-monocular condition. Expressed differently, it appears that we cannot treat two separate presentations to separate eyes as simply independent, to-be-summed events, as would be dictated by a simple, peripheral-threshold-only model. The peripheral a(t) curves overlap and push more area above the central a(t) threshold, whereas the two curves from the two pulses in a gap-monocular presentation cannot overlap. The extra area pushed above the central threshold predicts that dichoptic performance is slightly above gap-monocular performance.

A comparison of Busey and Loftus's (1994) Experiment 4, and the present Experiment 1 confirms this prediction: the difference between the dichoptic and monocular curves in the present Experiment 1 is not as great as the difference between the gap-monocular and monocular curves in Busey & Loftus's (1994) Experiment 4. Subtracting gap monoptic performance from monoptic

performance reveals that 20-25 percentage points separates the two conditions in Experiment 4 of Busey & Loftus (1994)[8]. However, subtracting dichoptic performance from monocular performance reveals only a 10-15 percentage point separation between the two conditions of Experiment 1. Monoptic performance was similar in the two experiments, never differing by more than 10% across experiments.

Although these findings suggest that gap monoptic performance is inferior to dichoptic performance, this conclusion requires an across-experiment comparison. In Experiment 2 we reconfirm this finding by comparing the three conditions (monocular, dichoptic and gap-monocular) in a single experiment. Thus Experiment 2 provides a further test of the dual-threshold model, along with independent estimates of the model parameters.

Experiment 2: Testing the Independent Sampling Model with Two Thresholds

From the perspective of the dual-threshold model, the fundamental difference between a dichoptic and a gap-monocular presentation is that the two peripheral a(t) curves of a dichoptic presentation are only processed independently up to the point where they combine to produce the central a(t) function. After this happens, the two peripheral a(t) curves overlap and sum to produce more area above the central a(t) threshold in a dichoptic presentation, and thus the model predicts greater dichoptic performance compared to a corresponding gap-monocular condition.

To see why this is, consider Figure 10. The left panel shows the central a(t) curve for a 150 ms monocular presentation, with the central a(t) threshold. The middle panel shows the central a(t) curve for a dichoptic presentation consisting of two 75 ms displays with a zero ISI. Even though the overall exposure duration is identical in the two conditions, the top of the dichoptic a(t) curve appears bowed when compared to the monocular curve. This happens because presenting all of the stimulus to the same eye as in a monocular presentation creates an a(t) curve that is wider above the a(t) threshold than the two dichoptic a(t) curves (see top panel of Figure 10, solid vs. dashed curves). This results in more above-peripheral-threshold area for the monocular condition. The bow in the dichoptic central a(t) function (middle panel, Figure 10) results from the narrower dichoptic peripheral a(t) curves, that tend to lose more area to the peripheral a(t) threshold.

INSERT FIGURE 10 ABOUT HERE

The right panel of Figure 10 shows the central a(t) curve for a gap-monocular presentation consisting of two 75 ms displays separated by a 250 ms ISI. This panel demonstrates the sensory

---

[8] The Busey & Loftus (1994) data were graphed using a nonlinear transformation of percent correct, but here we convert the Experiment 4 data back to percent correct to make this comparison.

independence between the two curves: the ISI is long enough to prevent the first presentation from summing with the second. Accordingly, there is less area above the central a(t) threshold, reducing performance for this condition compared to both the monocular and dichoptic conditions.

The two peripheral a(t) thresholds ensure that dichoptic performance is below monocular performance, but the interaction of the two dichoptic peripheral a(t) curves at the central a(t) curve drives more area above the central a(t) threshold. Thus dichoptic performance is predicted to be above the gap-monocular condition but below the monocular condition.

Predictions Summary

Let us summarize the predictions of Experiment 2. A finding of monocular performance above dichoptic performance implies a model with a peripheral threshold. A finding of dichoptic performance is above gap-monocular performance implies a central threshold.

Method

Experiment 2 incorporates three basic conditions. In the *monocular* condition a single d-ms stimulus was presented to one eye. In the *dichoptic* condition there were two (d/2)-ms stimulus presentations, the first to one eye and the second to the other eye, separated by a zero ISI. In the *gap-monocular* condition there were two (d/2)-ms presentations, both to the same eye, separated by a 250 ms ISI.

Observers, Stimuli and Apparatus

Observers, stimuli and apparatus were identical to those of Experiment 1, except that Observer TAK was replaced by TK, a male graduate student.

Design and Procedure

The design and procedure were essentially identical to those of Experiment 1 except that the binocular condition was replaced by the gap-monocular condition. There were 8 durations with each of the 3 conditions. Observers completed 18, 72-trial blocks, which provided 54 observations per condition per observer.

Results

Figure 11 shows the results of Experiment 2. Because there were qualitative differences between observer GW and the other two observers, we present individual data here. Observer TB's and TK's data (left and middle panels) confirm the foregoing prediction: dichoptic performance (filled squares) lies between monocular and gap-monocular performance. Observer TK's dichoptic data is close to the gap-monocular data, although dichoptic performance is significantly greater than the gap-monocular data, $t(1520) = 3.87$, $p < 0.0001$.

INSERT FIGURE 11 ABOUT HERE

Observer GW's data are shown in the right panel. The most important difference is that dichoptic and gap-monocular performance are the same. The dual-threshold model, however, can fit each data pattern with different parameter values. Consider the comparison between observer TB and Observer GW. Figure 12 shows the central a(t) curves for observers TB and GW for each condition, as generated by the best-fitting model parameters. The top three panels demonstrate why a dual-threshold model predicts dichoptic performance between the monocular and gap-monocular performances: the low peripheral threshold and the temporal proximity of the two peripheral a(t) curves combine to produce more above-threshold area relative to the gap-monocular condition.

INSERT FIGURE 12 ABOUT HERE

Observer GW's overall performance is approximately half that of the other two observers (possibly because GW, at age 50, was approximately twice as old as TB and TK). From the model's perspective, this is a direct result of a high peripheral a(t) threshold, causing a greater loss of area compared to observer TB. The bottom three panels of Figure 12 show the central a(t) curves given by the best-fitting model parameters for GW. A large peripheral threshold does not allow the two peripheral a(t) curves to overlap centrally as much. Without this large overlap, the two dichoptic curves will produce the about the same above-threshold area as the gap-monocular curve, and subsequently similar performance.

Because observer GW's dichoptic and gap-monocular performances were close together, a dual-threshold model with the central threshold set to zero (equivalent to the pure peripheral threshold model) will account for the data. However, the best fit to the data comes from peripheral and central a(t) thresholds that are both positive.

Observer TK's overall performance lies somewhere in between the other observers and he has a peripheral threshold that is in between TB’s and GW’s. We see a concomitant reduction in the difference between dichoptic and gap-monocular performance. However, this data pattern is readily accounted for by the theory. The parameter values for the three observers in Experiment 2 are listed in Table 2.

Discussion

Experiment 2 confirms the dual-threshold model, which is implied by Observer TB's and TK's data, and provides the best fit to Observer GW's data. In addition, the fit to Observer GW's data demonstrates how predictions that seem qualitatively different come from a single theory's different parameter values.

Experiment 3: Testing the Central Threshold

Experiments 1 and 2 have provided strong support for a peripheral threshold: monocular performance above dichoptic performance requires some form of pre-combination information loss.

This information loss is represented in the dual-threshold theory by a peripheral threshold. All three observers in Experiments 1 and 2 demonstrated a clear superiority for monocular over dichoptic performance. However, Experiment 2 provides only weak support for a central threshold; only two of the three observers (Observers TB and TK) demonstrates a difference between dichoptic and gap-monocular performance. Perhaps the conditions used in Experiment 2 were not powerful enough to distinguish between a theory that requires a central threshold and a theory that does not. One goal of Experiment 3 was to test the central threshold component of the theory directly.

To test the central-threshold component of the dual-threshold theory, Experiment 3 incorporates dichoptically presented stimuli, and variation in the interstimulus interval (ISI) between the two pulses of a dichoptic presentation. To see how this manipulation identifies the existence of a central a(t) threshold, consider a basic dichoptic presentation consisting of a 60-ms presentation to one eye followed by a 60-ms presentation of the same stimulus to the other eye. Consider two conditions that differ in the ISI between the two presentations. In the first condition, ISI is zero ms, while in the second condition it is 45 ms. Because the two conditions engender two identical peripheral a(t) curves, they both generate the same above-peripheral-threshold area passed to the combination mechanisms. As a result of these identical areas passed to the combination mechanism, any performance difference between the two conditions must be caused by post-combinatorial mechanisms; that is, a detrimental ISI effect must result from either a loss due to a central threshold or a loss in the combination of the two peripheral areas via nonlinear summation.

Figure 13 demonstrates the central a(t) curves resulting from monocular, 0-ms ISI dichoptic and 45-ms ISI dichoptic presentations, and demonstrates that a central-threshold assumption makes the prediction that as ISI increases, performance will decrease in the dichoptic condition.

INSERT FIGURE 13 ABOUT HERE

Method

Experiment 3 uses the monocular and dichoptic stimuli of Experiments 1 and 2. However, in the dichoptic condition the ISI between the first and second pulses was systematically varied from 0 to 90 ms. The duration of each of two pulses in each dichoptic presentation was either 30, 45, 60 or 75 ms.

Observers

Three observers participated in Experiment 3: the first author TB, a female graduate student LM, and a male graduate student MB.

Stimuli and Apparatus

The stimuli and apparatus were identical to those of Experiment 1. The contrast of the digits was set to 7.1%.

Design and Procedure

Both monocular and dichoptic stimuli were used. Within the dichoptic condition were 5 different ISI's ranging from 0 to 90 ms. The two pulses were the same duration, which was 30, 45, 60 or 75 ms. Within the monocular condition were 4 stimulus durations: 60, 90, 120 or 150 ms. Observers completed 24, 72-trial blocks, which provided 72 observations per condition per observer.

Results and Discussion

Experiment 3 results are summarized in Figure 14. All three observers produced data that demonstrate the same overall pattern, and thus averaged data are shown. The solid lines represent the dual-threshold model fit, whose best fitting parameters are provided in Table 2. Two findings in these data are noteworthy.

INSERT FIGURE 14 ABOUT HERE

First, as ISI is increased in the dichoptic condition, performance decreases. This implies some form of post-combinatorial information loss, as modeled by a central a(t) threshold in Figure 13. Prior to the combination of the information from each eye, dichoptic presentations with different ISI's all provide the same information; the ISI only becomes relevant once the responses from each eye are combined. However, under a linear-summation mechanism, increasing the ISI still cannot cause a decrease in performance without something like a central a(t) threshold, because the various dichoptic conditions have the same *overall* area under their central a(t) functions. The central threshold causes a reduction in performance for longer ISI dichoptic conditions because it tends to eliminate more of the area under the wider, shorter central a(t) curves produced by a longer ISI dichoptic condition. Thus under the current dual-threshold model conceptualization, the Figure-14 data imply a central a(t) threshold.

The second noteworthy finding in the Figure 14 data is that monocular performance is above the zero-ISI dichoptic condition's performance. This is most clearly evident for the short-duration presentations. Overall the magnitude of the effect is somewhat reduced when compared to the differences observed between these two conditions in Experiments 1 and 2. However, this pattern held for all three observers, with the exception of the longest-duration condition for Observer TB. The superiority of monocular performance in this as well as in Experiments 1 and 2, constitutes clear evidence for some form of pre-combinatorial information loss. Within the context of the dual-threshold model, this information loss implies a peripheral a(t) threshold.

Taken together the findings shown in Figure 14 confirm the dual-threshold model and reconfirm the existence of a post-combinatorial source of information loss, modeled within the theory as a central a(t) threshold.

To summarize the conclusions of Experiment 3, we have again disconfirmed a version of the linear-summation model that does not have some form of post-combinatorial information loss, and we have demonstrated that when this post-combinatorial information loss is modeled by a central a(t) threshold we can provide good quantitative fits to the data.

GENERAL DISCUSSION

It is generally agreed that two eyes are better than one. For some tasks, binocular superiority is implied by simple geometry: it is self evident, for instance, that binocular vision can aid in inferring the three-dimensional structure of the world. What is not so obvious, however, is that binocular vision also helps when simple, two-dimensional visual information is all that is required to perform the task at hand, as is the case in our digit-recall task. This means that information must somehow be acquired faster with two eyes than with only one eye. We have described a theory that accounts for such speedup. This theory includes sensory thresholds that affect monocular performance more than binocular performance. In what follows, we make several remarks about the thresholds in particular, along with general implications of our threshold notions for interpreting binocular superiority. Note that it is not our intent to provide a complete model of binocular combination that accounts for the wide variety of phenomenon that exist in the binocular combination literature. Rather, we have embedded a somewhat simplified binocular combination model within our general theory. This model is designed to (1) illustrate the implications of the sensory threshold, (2) examine the mechanisms of binocular combination in conjunction with this threshold, and (3) demonstrate the role of temporal interactions that result from overlapping sensory-response functions.

Above-Probability Summation Performance does not Implicate Neural Interaction

In their review of the binocular-summation literature, Blake and Fox (1973; see also Blake, Sloane & Fox, 1981) suggested that binocular performance above that predicted via probability summation from monocular performance implies "genuine neural interaction between the eyes, not just probability summation" (Blake et al., 1981, p. 266). We conclude that this need not be the case: we have provided a model that makes an above-probability summation prediction with a linear-summation mechanism. The existence of a post-combinatorial information loss (modeled by the central threshold) is completely responsible for this prediction.

Consider the bottom panel of Figure 5. In the absence of a central threshold, the binocular curve is twice as high as a same-duration monocular curve (with or without a peripheral threshold); correspondingly, the binocular-curve area is twice as great as the monocular-curve area. In the absence of additional mechanisms, this would fulfill a probability-summation prediction of $p_B = 2p_M - p_M^2$. However, when a central a(t) threshold is introduced, binocular performance rises

above what would be predicted from probability summation. This happens because the monocular curve's lower height renders it more vulnerable to a central a(t) threshold than a binocular curve. From this perspective, binocular performance is observed to be above what is predicted by probability summation not because observers are doing *better* in the binocular task, but because they are doing *worse* in the monocular task. They are doing worse as a direct result of a post-combinatorial information loss, that differentially affects monocular performance more than binocular performance, not because of a greater-than-linearity summation mechanism.

Alternative Ocular-Channel Combination Models

An explicit assumption of the current linear-summation model is that the above-threshold areas from the two monocular channels simply *sum* to produce the central a(t) function, upon which performance is based. While this combination mechanism has support from neuroscience (Ohzawa & Freeman, 1986) and has been adopted by Legge (1984 a, b) and others, alternative mechanisms have been proposed. We would like to consider in detail a model developed by Alexander Cogan (Cogan, 1987; 1990). A summary of this model is below; a more complete description is found in Figure 15. We have adapted this model to the current data, and we discuss the extensions to the model that are required to account for the present experimental data.

INSERT FIGURE 15 ABOUT HERE

The Cogan model assumes that the two eyes perform transduction on incoming stimuli to produce ipsilateral excitation (e_L, e_R) and contralateral inhibition (i_L, i_R). The amount of inhibition is proportional to the excitation, such that $i_R = c \bullet e_L$ and $i_L = c \bullet e_R$. The combined either-eye output, b_x is given by:

$$b_x = \frac{e_R}{(1 + c\ e_L)} + \frac{e_L}{(1 + c\ e_R)} \qquad \text{Eq. 13}$$

A separate, fused channel, b_F, is given by:

$$b_F = k\ e_R\ e_L \qquad \text{Eq. 14}$$

and the net binocular effect is simply the sum of b_x and b_F.

Components of this model share similarities with the Dual-Threshold model presented here. Cogan et al. (1990) developed a linear-filter front end and used this model to fit two-pulse detection thresholds, in which the two pulses could either be the same contrast (++) or opposite contrast (+-). They systematically varied the stimulus onset asynchrony (SOA) and determined relative sensitivities to each type of stimulus. Although they did not obtain quantitative model fits, qualitative model predictions corresponded to the observed data.

Two-pulse stimuli like those used in the 1990 paper provide good estimates of the parameters of linear filters (Busey, 1994). Due to the qualitative success of the Cogan model to account for the two-pulse data, we fit the Cogan model to the present data. Before describing the results of this modeling, some comparisons between the two models are in order.

A major emphasis of the present work is the effects of post-combinatorial information loss on binocular and monocular stimulus representations. An example is the ability of the Dual-Threshold model with a central sensory threshold to account for above-probability-summation binocular performance, even with a linear summation combination mechanisms. This results from the higher binocular central a(t) function that allows more area to survive a central sensory threshold. The binocular channel b_F in the Cogan model can in principle have the same effect: if both e_L and e_R are active at once, b_F will be large, giving a larger response and thus better performance. This is qualitatively similar to the two peripheral a(t) curves providing more above-central-threshold area when they co-occur. Thus the free parameter k from Cogan's binocular channel is somewhat analagous to the free parameter Θ_c in the Dual-Threshold model.

The interocular inhibition from the Cogan model serves to reduce the response in the opposite monocular channel. This pre-combinatorial information loss is somewhat analagous to the peripheral thresholds in the Dual-Threshold model. There are important differences, in that the peripheral thresholds act only on a single monocular channel, which the interocular inhibition crosses channels. However, within the model formulations, pre-combinatorial information loss is represented by a single free parameter, either c or Θ_P.

Qualitatively, the Dual-Threshold model and the Cogan model are similar and have the same number of free parameters, although perhaps the added complexity of the Cogan model gives it more explanatory power. Given this, it is reasonable to ask whether the Cogan model can fit the data from Experiments 1-3. Such fits require an information-processing model component to deal with the change from a detection paradigm to a letter identification paradigm.

To assist in model comparison, we simply appended the information-processing mechanisms of the Dual-Threshold model to the output of the Cogan model (Eq 7). Consistent with the Dual-Threshold model, we assumed that the presentations to each eye engenders a peripheral sensory response function corresponding to Cogan's e_L or e_R. These two response functions inhibit each other in proportion to their height at each moment in time, according to the free parameter c. A separate binocular channel was also created from the peripheral sensory response functions according to the free parameter k according to Eq 14. The sum of these two channels gives a central sensory response function. The area of this central sensory response function is used to generate a performance prediction via Eq. 7.

Surprisingly, the Cogan model could not fit the data as well as the Dual-Threshold model, despite the added complexity of the model. Parameter values are shown in Table 3. The left panels of Figure 16 show the fits to the averaged data from Experiments 1 and 3. The data from Experiment 2 could also not be fit, but are not shown, since the conclusions derived from the data mirror those from Experiment 1. The reason for these poor fits appears to come from a binocular excitation channel that cannot completely take the place of a central information loss that accounts for both the above-probability-summation binocular performance of Experiment 1 and the decrease in performance with increasing ISI from Experiment 3. When a central nonlinearity such as a central threshold is added to the Cogan model (Figure 16, right panels), the revised Cogan model gives very good fits in all cases. However, the addition of a central threshold gives the revised model one more free parameter that the Dual-Threshold model.

INSERT FIGURE 16 ABOUT HERE

INSERT TABLE 3 ABOUT HERE

To summarize, while the Experiment 1-3 data disconfirm the simple version of the Cogan model, the model gives excellent quantitative fits if a central threshold or central power function is added. Such an addition might be required by the additional complexity of the task: detection and letter identification might require different spatial and temporal frequencies (Busey, 1994) and letter identification is best thought of as a classification task. The central information loss may result from inefficiencies or noise in the information processing mechanisms that are not required for simple detection.

Evidence for Temporal Inhibition

The impulse response function used in the present work (Eq. 1) is *monophasic*, and therefore does not allow for temporal inhibition. Busey (1994) found weak evidence for temporal inhibition in related tasks, and when the theory was modified to include temporal inhibition (via a biphasic impulse response function, setting $s>0$ in Eq. 1) it successfully accounted for the data in these related tasks. However, application of this biphasic model to the present data did not markedly improve the fit over that provided by the monophasic model that we have described (despite two additional free parameters). This failure result from the peripheral thresholds, the effects of which tend to eliminate the inhibitory components of the biphasic peripheral a(t) curves. Similarly, a version of the theory that includes temporal inhibition but without peripheral a(t) thresholds also did not provide a markedly better fit to any of the three data sets. A version of the Cogan model with temporal inhibition did not provide fits better than those shown in Figure 16, despite requiring two additional free parameters.

Neuroscience Evidence for a Central Threshold

Using single-cell recording in cat, Ohzawa & Freeman (1986) found overwhelming evidence for linear summation in binocular cells. However, a minority of cells exhibited deviations from this linearity, in that the response from the cell was maximal when both eyes were equally stimulated, but dropped off at a rate faster than would be expected from a linear model when one eye was reduced. This is quite similar to the behavior of the central threshold observed in the current modeling (e.g. Figure 13). Indeed, Ohzawa & Freeman attribute this nonlinearity to a threshold mechanism that comes into play after the linear binocular summation. One possible mechanism for such a threshold is the threshold for firing on the post-synaptic cell receiving input from both eyes. Weak stimulation to either eye may not exceed this threshold and cause the cell to fire, although weak stimulation to both eyes may result in an action potential on the post-synaptic cell.

The importance of a post-combination threshold mechanism has been demonstrated in other domains as well. For example,

get full paper and see if relevant

Sensory Thresholds: Implications for Cognitive Psychologists

As noted above, the notion of peripheral and central a(t) thresholds is similar to peripheral and central sources of noise. Denis Pelli (personal communication) has demonstrated that under some conditions, either the central or peripheral noise dominates the signal, and thus affects performance. He and Manoj Raghavan (Pelli, Raghavan & Ahuja, 1995; Raghavan & Pelli, 1995) demonstrate that the visibility of large, long-duration letters is limited by (central) cortical noise, and that visibility of small, brief-duration letters is limited by (peripheral) photon noise. The important implication for perception researchers is that a stimulus variable such as size can differentially affect two stages of processing (peripheral or central). Thus these two stages become important to model even in experiments that do not use monocular or dichoptic stimuli.

The thresholds as conceptualized above may be thought of as a constant drain on a system that is attempting to process a signal. Consider a metaphor in which the a(t) function represents the speed of some system, say the value of the speedometer in a car. The total amount of information, i.e. the area under the a(t) function, is analogous to the odometer reading after some period. Once the threshold is added, however, the metaphor changes to a motorboat traveling upriver. The speed of the current represents the height of the threshold; thus if motorboat speed does not exceed the current speed, then no upriver progress will be made.

Conclusions

We have extended a previously proposed theory of visual information processing to the domain of binocular combination. Application of this extended theory to data from three

experiments helps identify the sources of information loss, both pre- and post-combination. Finally we have confirmed a version of the extended theory that combines both pre- and post-combinatorial sources of information loss with a linear-summation combination mechanism and an independent sampling information acquisition mechanism. This application demonstrates that the question of the combination mechanisms involved in binocular combination is intimately tied to the question of pre- and post-combination sources of information loss: one cannot simply look at monocular and binocular data and infer the combinatorial mechanisms without also considering the potential for something like peripheral and central sensory-response thresholds. In particular, the existence of a central threshold implies that binocular performance above a probability summation prediction based on monocular data need not implicate an above-linear-summation combination mechanism. A linear summation mechanism and a central threshold will provide an equivalent account.

The linear-filter model components also allows a good quantitative account of the degree to which the relationship between monocular and binocular performance changes as the asynchrony between the two pulses of the binocular stimulus changes. Such modeling reveals not only under what conditions the two monocular channels influence each other, but how they are affected by the post-combinatorial information loss. Finally, we have demonstrated that such quantitative fits are important when comparing two models that have similar structure and components and thus give qualitatively similar results.

References

Ames, C. & Palmer, J. (1992). *Macintosh Experimental Software*. Seattle, WA: unpublished computer code.

Blake, R. & Fox, R. (1973). The psychophysical inquiry into binocular summation. *Perception & Psychophysics, 14,* 161-185.

Blake, R., Slone, M. & Fox, R. (1981). Further developments in binocular summation. *Perception & Psychophysics, 30,* 266-276.

Busey, T. A. (1994). Temporal Inhibition in Two-Pulse Character Detection and Identification Tasks. University of Washington, August, 1994.

Busey, T.A. & Loftus, G.R. (1994). Sensory and cognitive components of visual information acquisition. *Psychological Review , 101,* 446-469.

Cogan, A. (1987). Human binocular interaction: Towards a neural model. *Vision Research, 27,* 2125-2139.

Eriksen, C. W., & Greenspon, T. S. (1968). Binocular summation over time in the perception of form at brief durations. *Journal of Experimental Psychology, 76,* 331-336.

Eriksen, C. W., Greenspon, T. S., Lappin, J. & Carlson, W. A. (1966). Binocular summation in the perception of form at brief durations. *Perception & Psychophysics, 1,* 415-419.

Green, D., & Swets, J. (1966). *Signal detection theory and psychophysics*. New York: Wiley.

Green, D., & Swets, J. (1974). *Signal detection theory and psychophysics*. Huntington, NY: Robert E. Krieger.

Julesz, B. (1971). *Foundations of Cyclopean Perception*. Chicago, IL: University of Chicago Press.

Legge, G. (1984a). Binocular contrast summation-I. Detection and discrimination. *Vision Research, 24,* 373-383.

Legge, G. (1984b). Binocular contrast summation-II. Quadratic summation. *Vision Research, 24,* 385-394.

Loftus, G. R., Busey, T.A. & Senders, J. (1993). Providing a sensory basis for models of visual information acquisition. *Perception & Psychophysics, 54,* 535-554.

Loftus, G. R., Duncan, J. & Gerhig, P. (1992). On the time course of perceptual information that results from a brief visual presentation. *Journal of Experimental Psychology: Human Perception and Performance, 18,* 530-549.

Loftus, G.R. & Irwin, D.E. (1995). Visible persistence and iconic storage are different, but related things. Cognitive Psychology (under revision).

Loftus, G.R. & McLean, J. A theory of the information acquisition that underlies picture recognition (in preparation).

Loftus, G.R. & Ruthruff, E.R. (1994). A theory of visual information acquisition and visual memory with special application to intensity-duration tradeoffs. *Journal of Experimental Psychology: Human Perception and* Performance, 20, 33-50.

Massaro, D.W. (1970). Perceptual processes and forgetting in memory tasks. *Psychological Review*, 77, 557-567.

Matin, L. (1962). Binocular summation at the absolute threshold of peripheral vision. *Journal of the Optical Society of America, 52*, 1276-1286.

Ohzawa, I., & Freeman, R. D. (1986). The binocular organization of simple cells in the cat's visual cortex. *Journal of Neurophysiology, 56*, 221-242.

Pelli, D. G., Raghavan, M. & Ahuja, S. (1995) The noises that limit visual perception. Paper presented at the 1995 Association for Research in Vision and Ophthalmology Conference.

Raghaven, M., & Pelli, D. G. (1995) Psychophysical evidence for cortical noise. Paper presented at the 1995 Association for Research in Vision and Ophthalmology Conference.

Rumelhart, D.E. (1970). A multicomponent theory of the perception of briefly exposed visual displays. *Journal of Mathematical Psychology, 7*, 191-218.

Shibuya, H., & Bundesen, C. (1988). Visual selection from multielement displays: Measuring and modeling effects of exposure duration. *Journal of Experimental Psychology: Human Perception and Performance, 14*, 591-600.

Sperling, G. & Melchner, M.J. (1978). Visual search, visual attention, and the attention operating characteristics. In J. Requin (Ed.) *Attention and Performance VII.* Hillsdale, N.J.: Erlbaum.

Sperling, G., & Sondhi, M.M. (1968). Model for visual luminance discrimination and flicker detection. *Journal of the Optical Society of America, 58*, 1133-1145.

Townsend, J. T. (1981). Some characteristics of visual whole report behavior. *Acta Psychologica, 47*, 149-173.

Watson, A. (1979). Probability summation over time. *Vision Research, 19*, 515-522.

Watson, A. B. (1986). Temporal sensitivity. In K. R. Boff, L. Kaufman, and J.P. Thomas (Eds.), *Handbook of Perception and Human Performance (Vol I)* New York: Wiley.

Westendorf, D. & Blake, R. & Fox, R. (1972). Binocular summation of equal energy flashes of unequal duration. *Perception & Psychophysics, 12*, 445-448.

Appendix A- Equations for All Model Fits

Parameter fitting was accomplished using a simplex gradient descent method. To avoid the possibilities of local minima, we computed the best fitting parameters multiple times, each time from a different starting location in parameter space. The vast majority of parameter searches terminated at the same ending parameters for a given model fit.

All model fits derive the peripheral sensory response functions, $a_p(t)$, via the convolution of the stimulus wave form with the impulse-response function of the linear filter:

$$a_p(t) = f(t) * g(t) \qquad \text{Eq. A1}$$

were g(t) is the gamma function from Eq 1. Note that for monocular and dichoptic stimuli, the left and right-eye f(t) functions will differ according to which eye is stimulated (or stimulated first in the dichoptic case).

Predictions for the Dual-Threshold Model

A peripheral threshold, Θ_p, is assessed on the peripheral a(t) wave form:

$$a_{\Theta,p}(t) = \begin{cases} a_p(t) - \Theta_p & (a(t) > \Theta_p) \\ 0 & (a(t) \le \Theta_p) \end{cases} \qquad \text{Eq. A2}$$

for the hard threshold version of the theory, or a power function is applied to the peripheral a(t) wave form:

$$a_{\beta,p}(t) = [a_p(t)]^{\beta} \qquad \text{Eq. A3}$$

The two peripheral sensory response functions sum to create the central sensory response function, $a_c(t)$:

$$a_c(t) = a_{\theta,L}(t) + a_{\theta,R}(t) \qquad \text{Eq. A4}$$

or

$$a_c(t) = a_{\beta,L}(t) + a_{\beta,R}(t) \qquad \text{Eq. A5}$$

for the power function version of the theory.

In the Dual-Threshold model, a central threshold is assessed to create $a_{\Theta,c}(t)$:

$$a_{\Theta,c}(t) = \begin{cases} a_c(t) - \Theta_c & (a_c(t) > \Theta_c) \\ 0 & (a_c(t) \le \Theta_c) \end{cases} \qquad \text{Eq. A6}$$

for the hard threshold version of the theory, or a power function is applied to the central a(t) wave form:

$a_{\beta,c}(t) = [a_c(t)]^{\beta}$ Eq. A7

The area under the $a_{\theta,c}(t)$ function is converted to performance via the following formula:

$p = 1.0 - e^{-A_{\Theta,c}(\infty)/c_s}$ Eq. A8

For the power-function version of the theory, performance is a function of the area under the $a_{\beta,c}(t)$ wave form:

$p = 1.0 - e^{-A_{\beta,c}(\infty)/c_s}$ Eq. A9

Predictions for the Cogan Model

Using the notation of the Busey & Loftus (1994) model, the Cogan model is formulated as follows:

$$b_x(t) = \frac{a_R(t)}{(1 + c\ a_L(t))} + \frac{a_L(t)}{(1 + c\ a_R(t))}$$ Eq. A10

and

$b_F(t) = k\ a_R(t)\ a_L(t)$ Eq. A11

where $a_R(t)$ and $a_L(t)$ represent e_R and e_L respectively. The central sensory response function $a_c(t)$ is computed via:

$a_c(t) = b_x(t) + b_F(t)$ Eq. A12

If a central threshold is applied after the point of combination, this formulation is added to create $a_{\Theta,c}(t)$:

$$a_{\Theta,c}(t) = \begin{cases} a_c(t) - \Theta_c & (a_c(t) > \Theta_c) \\ 0 & (a_c(t) \le \Theta_c) \end{cases}$$ Eq. A13

for the hard threshold version, or a power function is applied to the central a(t) wave form:

$a_{\beta,c}(t) = [a_c(t)]_{\beta}$ Eq. A14

In all three cases, performance is converted from the area under the central sensory response function via Eq 7:

$p = 1.0 - e^{-A_c(\infty)/c_s}$ Eq. A15

were $A_c(\infty)$ is replaced by $A_{\theta,c}(\infty)$ when a central threshold is added or by $A_{\beta,c}(\infty)$ when a central power function is added.

Author Note

This research was supported by an NIMH predoctoral fellowship to Thomas Busey and an NIMH grant to Geoffrey Loftus. We would like to thank George Wolford for many helpful comments concerning the interpretation and modeling of these data.

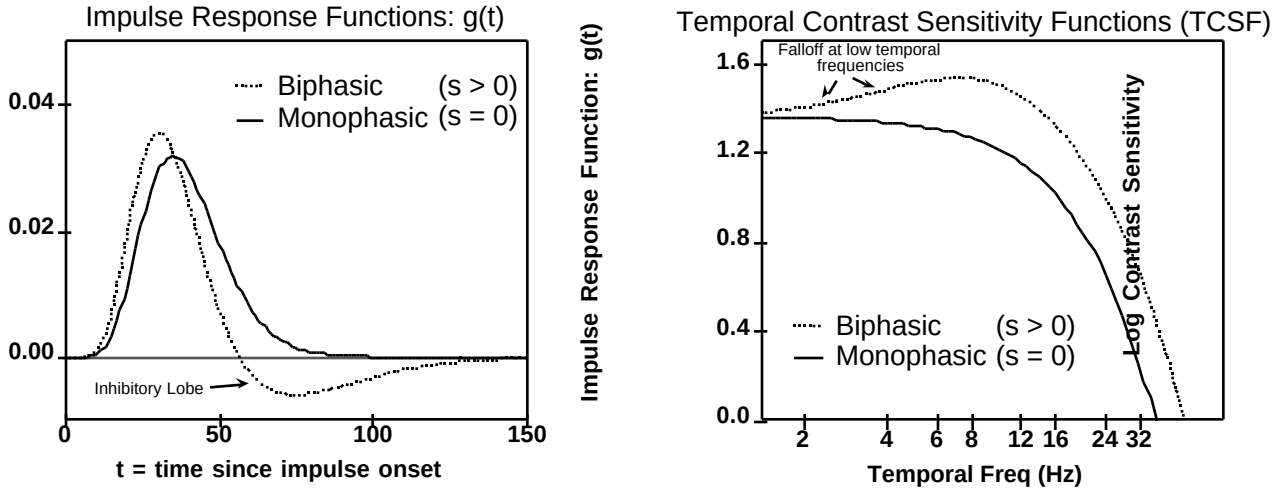

Figure 1. The temporal frequencies underlying a task may be characterized by an impulse response function (left panel) that characterizes the time course of the perceptual response engendered by a stimulus, or by the temporal contrast sensitivity function (right panel), that characterizes the fidelity by which the pathways subserving a given task pass different temporal frequencies. The TCSF plots are the Fourier transform of the impulse response functions into frequency space. High spatial frequency stimuli tend to elicit monophasic impulse response functions, which have no falloff at low temporal frequencies in the TCSF plot. Stimuli containing low spatial frequencies tend to elicit biphasic impulse response functions that contain an inhibitory lobe. This temporal inhibition acts to sharpen the response of the visual pathway, allowing it to respond to faster changes in the visual scene. However, this inhibition causes in a falloff at low temporal frequencies in the TCSF plot, which results from tendency for the biphasic impulse response function to inhibit itself when processing slow temporal changes. Parameters used: Monophasic: {$\tau = 4.38$, $r = 0$} Biphasic: {$\tau = 3.58$, $r = 2.0$, $s = 0.39$}

Figures

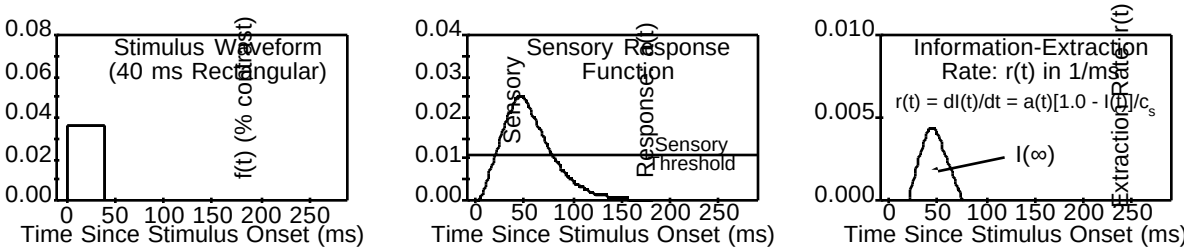

Figure 2. Theoretical components of the linear filter model of character identification. Left Panel: A stimulus is characterized by its changes in contrast over time. Middle Panel: The stimulus engenders a response in the visual system that is a function of the stimulus input function f(t) and the impulse response function g(t). A sensory threshold is assessed, such that further information processing does not proceed unless the sensory response exceeds the sensory threshold. Right Panel: If the sensory response exceeds the threshold, further information processing takes place at a rate defined by r(t). This rate is proportional to the product of the above-threshold sensory response and the proportion of remaining stimulus information. Performance in terms of proportion correctly-recalled digits is assumed to be proportional to the area under the information-acquisition rate function (which represents total acquired information).

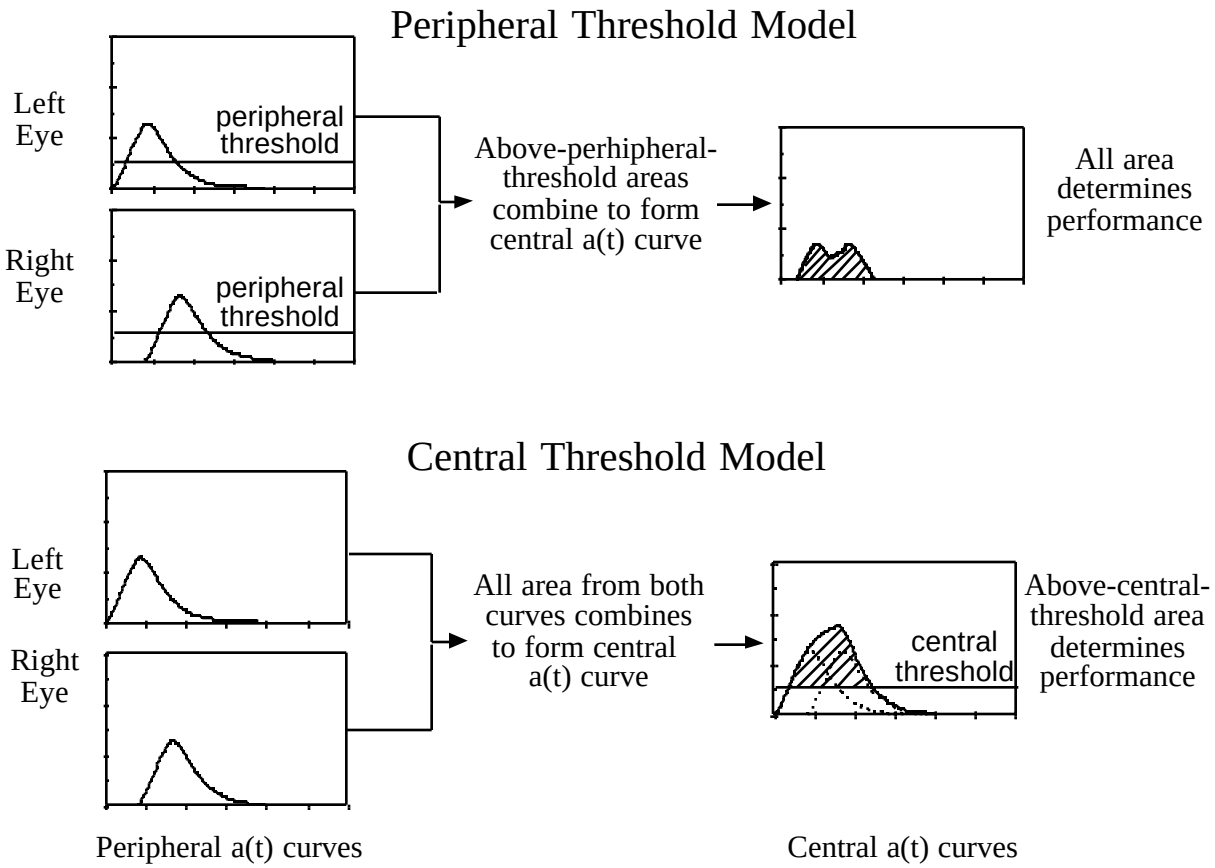

Figure 3. The peripheral and central-threshold models, along with the responses generated by a dichoptic presentation. Peripheral Threshold Model: Information enters each eye and engenders two *peripheral a(t) curves*. These curves pass through the *peripheral threshold*, Θ_P, such that only the above-peripheral-threshold area combines centrally to form the *central a(t) curve*. All of the area under this function determines performance. Central-threshold Model: The two presentations engender two peripheral a(t) curves, but under the central-threshold model all of the peripheral area combines centrally. After combination a *central a(t) threshold*, Θ_c, is assessed, such that only the above-central-threshold area determines performance.

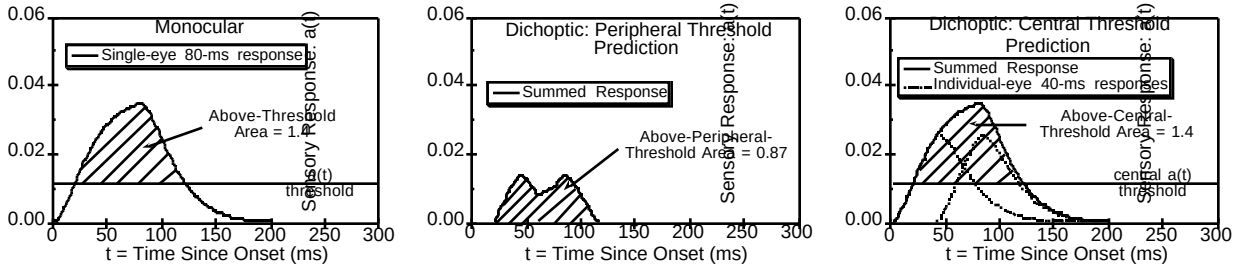

Figure 4. Left panel: a(t) function for a monocular d-ms presentation. Middle panel: Peripheral-threshold model's prediction for dichoptic presentation which gives less area and thus reduced performance compared to the monocular condition. Right panel: Central-threshold model's prediction for dichoptic presentation, which is identical to the monocular prediction and thus dichoptic performance will be identical to monocular performance.

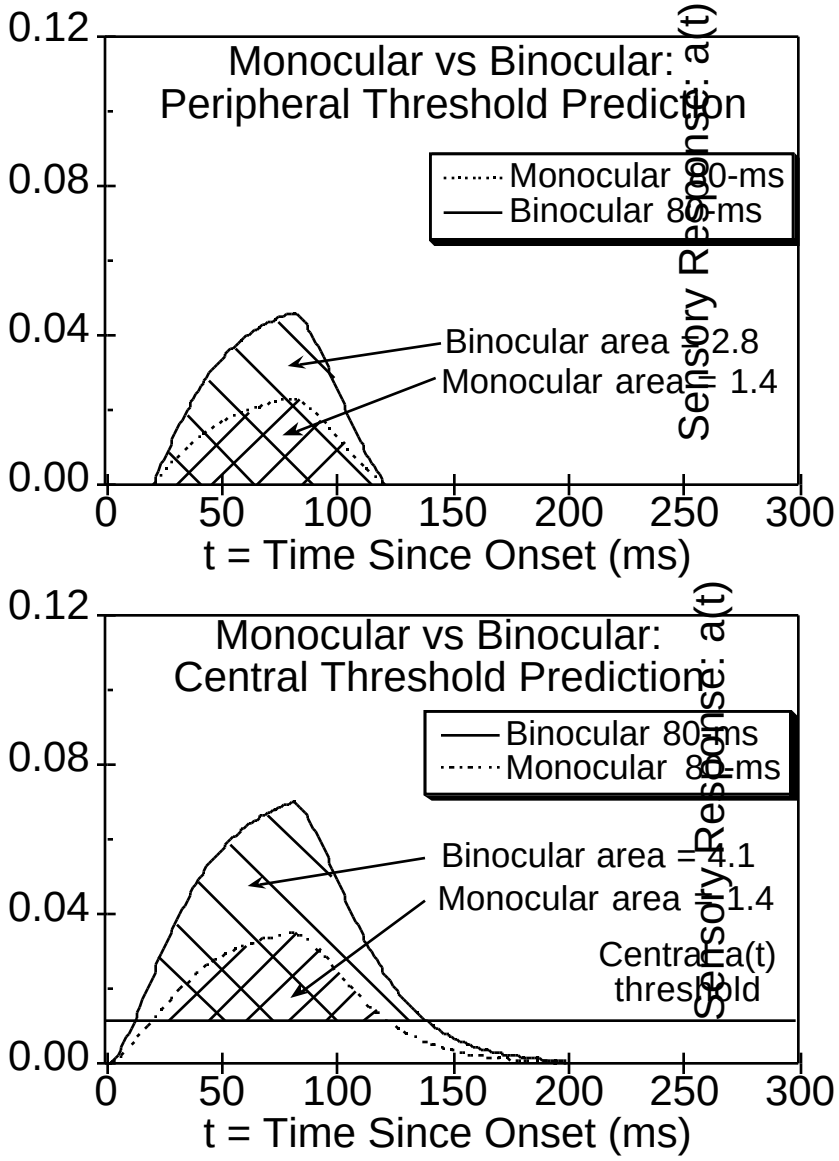

Figure 5. Top panel: Binocular and monocular central a(t) curves under a peripheral threshold model. The binocular area is always twice as great as the associated monocular area, and thus binocular and monocular performances obey a probability summation prediction: $p_B = 2p_M - p_M^2$. Bottom panel: Binocular and monocular central a(t) curves under a central-threshold model. Again the binocular curve is twice as tall as a monocular curve, but the central a(t) threshold affects the monocular area proportionately more. This causes a failure of probability summation because binocular performance would be predicted to be greater than that expected from a probability summation prediction based on monocular performance: $p_B > 2p_M - p_M^2$. Under an extreme case, the monocular curve might not even reach the central a(t) threshold, although a binocular might. In this case, $p_M = 0$ while $p_B > 0$, which is a clear failure of probability summation.

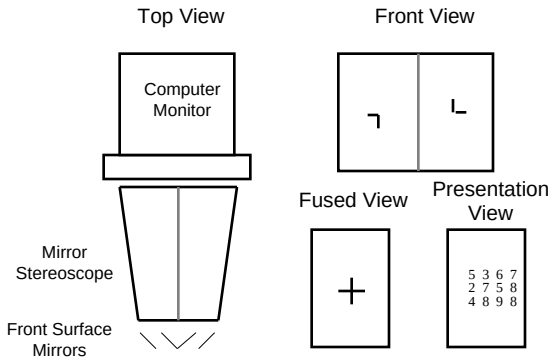

Figure 6. Display apparatus used in Experiments 1-3. Care was taken at the start of a block of trials to fuse the two "L's" into a cross to ensure that during the presentation view the digits overlapped on the same retinal area. The fixation point never disappeared, allowing maintenance of the fused condition.

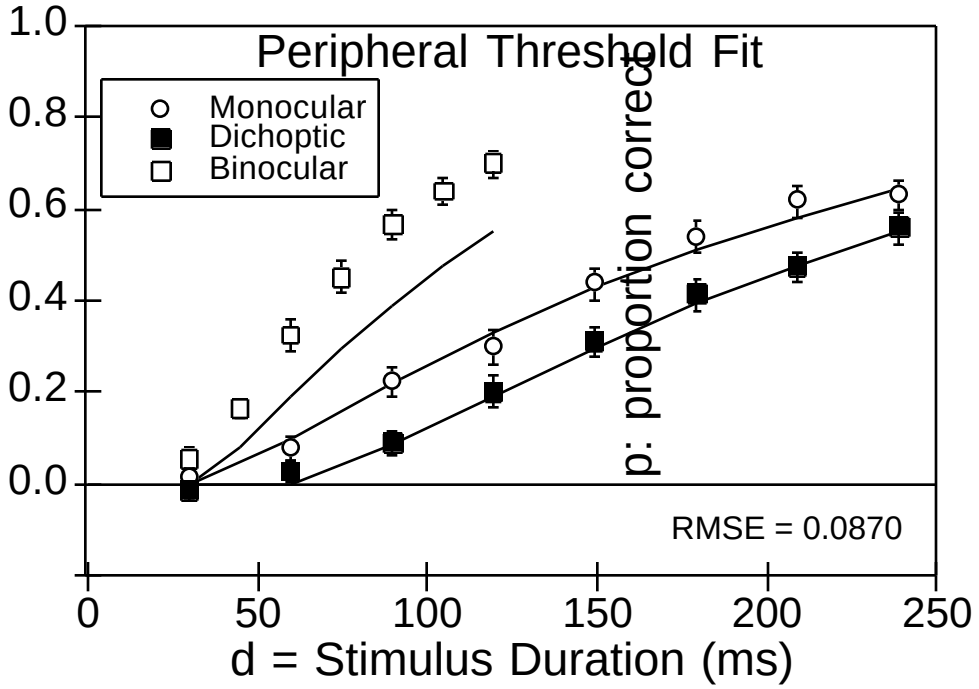

Figure 7. Experiment 1 results: data averaged for three observers, along with best-fitting predictions of the peripheral threshold model. For illustrative purposes, the model fit given in Figure 7 minimizes error around only the monocular and dichoptic presentations. This demonstrates the inadequacy of the probability summation assumption, implicit in the peripheral-threshold model, to describe binocular performance based on monocular performance.

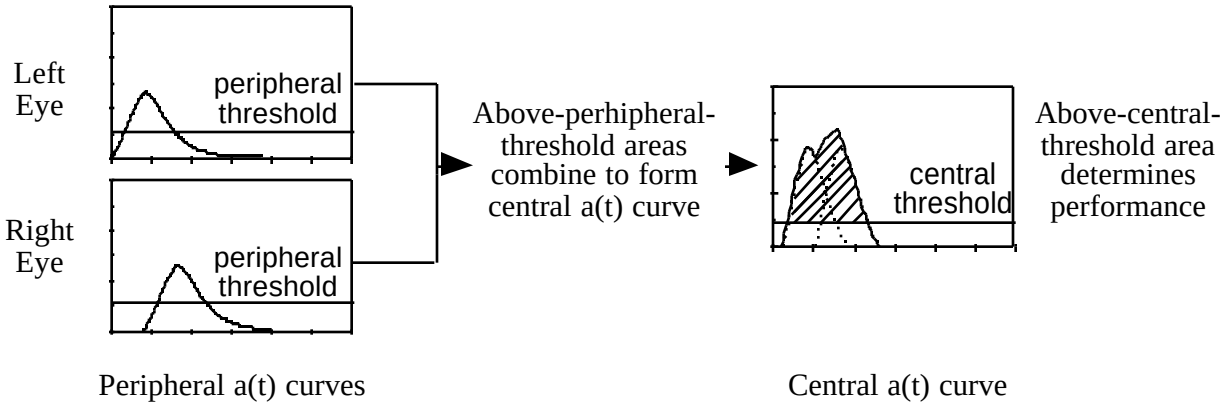

Figure 8. The dual-threshold model. Above-peripheral-threshold area from the peripheral a(t) curves combines to produce the central a(t) curve.

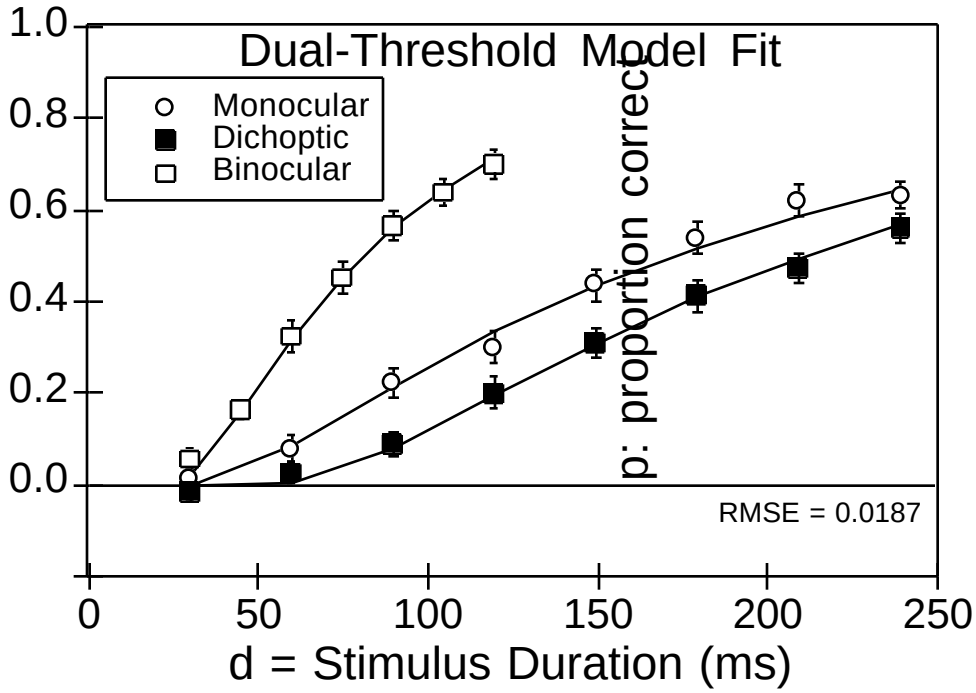

Figure 9. Experiment 1 results. Data are averaged for three observers; the solid line shows the best fit of the dual-threshold model to the averaged data.

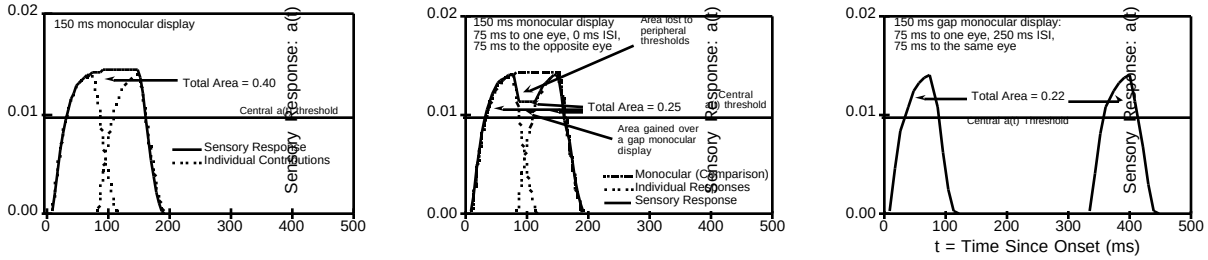

Figure 10. Left panel: Central a(t) curve for a 150 ms monocular presentation. Middle panel: Central a(t) curve for a 150 ms dichoptic presentation. Right panel: Central a(t) curve for a 150 ms gap-monocular presentation. The dichoptic and gap-monocular curves have less above-central-a(t) threshold area than the monocular curve, predicting lower performance for the dichoptic and gap-monocular conditions. However, the dichoptic area is slightly greater than the gap-monocular area, which implies that dichoptic performance will be slightly above the gap-monocular performance.

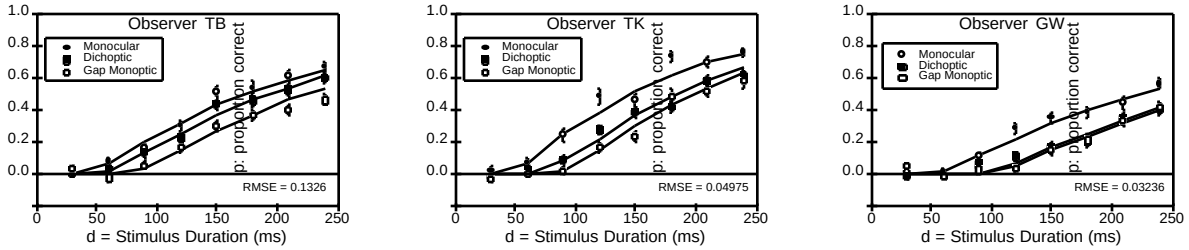

Figure 11. Experiment 2 results. Data for three separate observers along with best fits from the dual-threshold model.

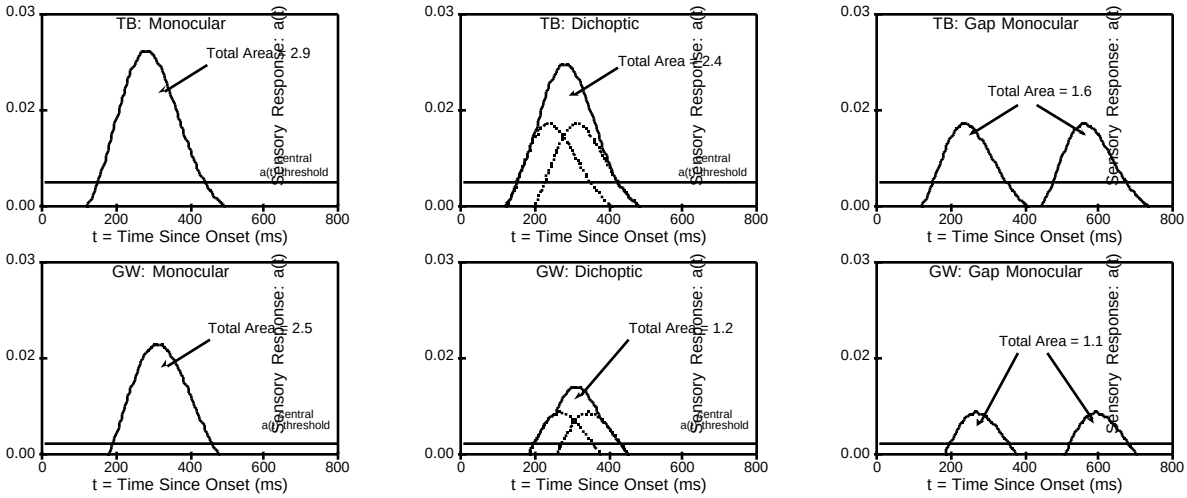

Figure 12. Central a(t) curves for Experiment-6 observers TB and GW, showing how different model parameters generate "qualitatively different" predictions with the same theory. GW's large peripheral thresholds allow less overlap of the peripheral dichoptic curves (middle panel) and thus they do not provide much more above-central-threshold area than the above-central-threshold area derived from the gap-monocular condition.

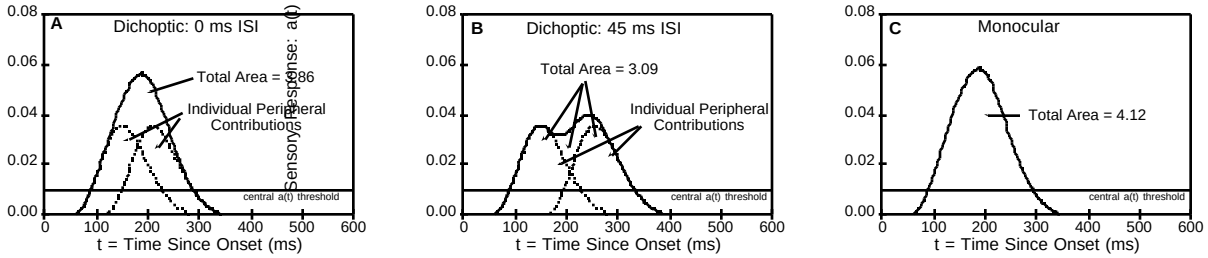

Figure 13. Linear-Summation dual-threshold Model. Central a(t) curves for 0-ms ISI dichoptic, 45-ms ISI dichoptic and monocular presentations for a 60 ms/60 ms condition. The two dichoptic condition central a(t) curves have the same *overall* area (panels A and B), because the individual peripheral contributions are the same for both conditions. However, because the 45 ms ISI dichoptic condition has area that is more spread out in time, the central threshold affects it more giving it less above-central-threshold area (3.86 vs. 2.09). This leads to the prediction that as ISI is *increased* in the dichoptic condition, performance will *decrease.* This decrease is solely due to the central a(t) threshold because the peripheral a(t) thresholds affect both pulses equally in all conditions. The right panel shows the curve resulting from a monocular presentation; the monocular area is slightly larger than the 0-ms ISI dichoptic area because the taller peripheral a(t) curve for the monocular condition puts more area above the peripheral a(t) threshold. The combination of peripheral and central threshold leads to the prediction that monocular performance will be above the 0-ms ISI dichoptic performance (as was seen in Experiments 1 and 2), and that performance will decrease as ISI is increased in the dichoptic condition.

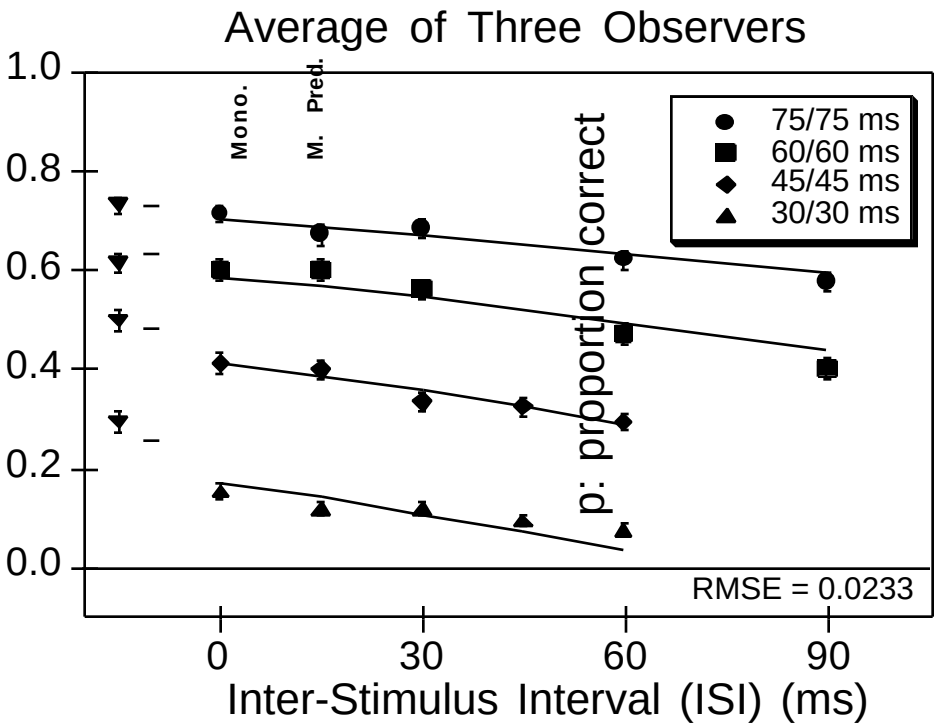

Figure 14. Experiment 3 results. Data are averaged for three observers; the solid line shows the best fit of the dual-threshold model with a linear combinatorial mechanism. The data show two important features. First, as ISI increases, performance in the dichoptic condition decreases. This finding provides evidence for a post-combinatorial information loss, modeled within the theory as a central a(t) threshold. Second, Monocular performance is above the zero-ISI dichoptic condition's performance, most markedly at the short-duration presentations of 30/30 ms and 45/45 ms. This provides evidence for a pre-combinatorial information loss, modeled within the theory as a peripheral a(t) threshold.

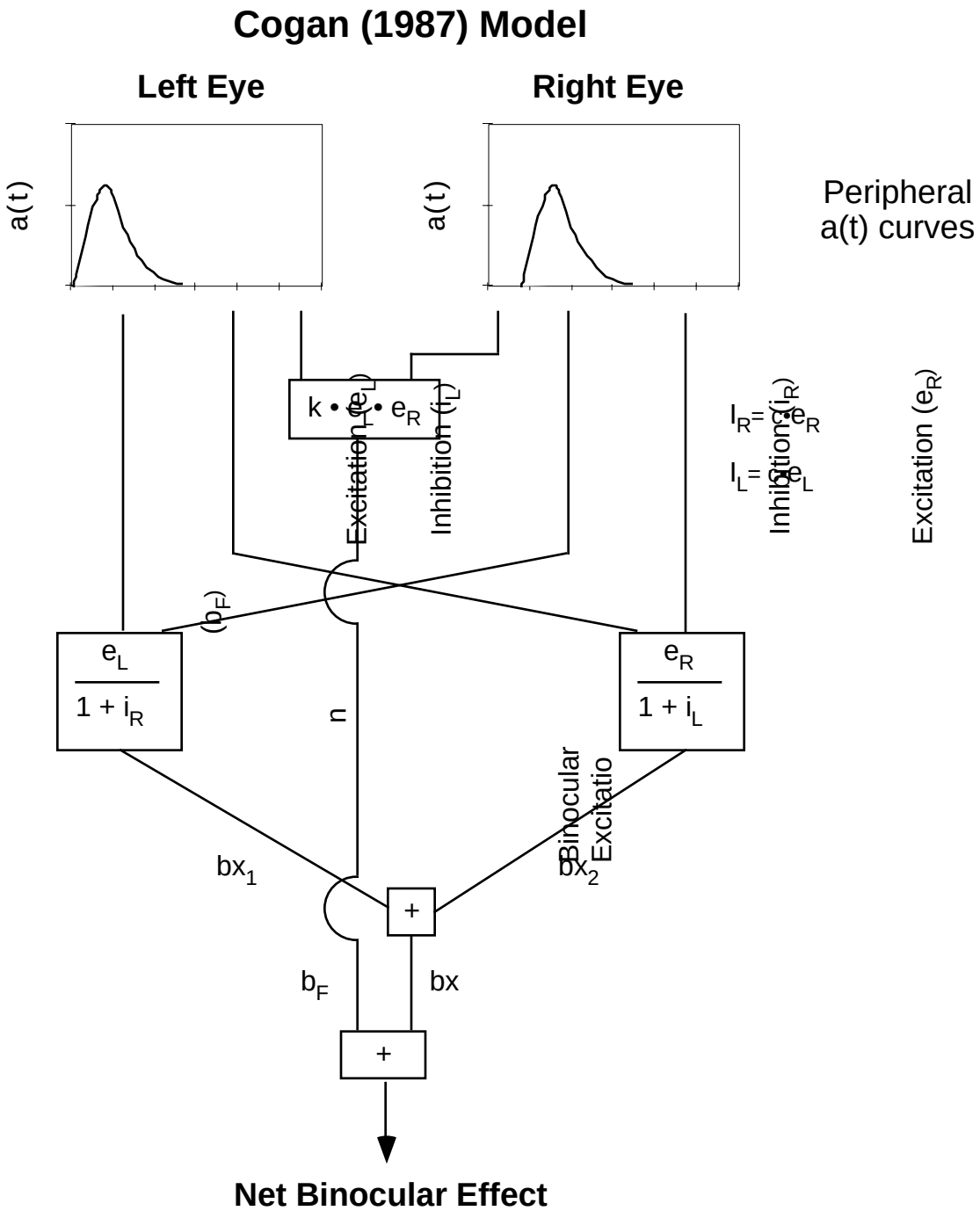

Figure 15. Cogan (1987) model applied to the Experiment 1-3 data. The height of the peripheral a(t) curves a each point in time is used to construct a Net Binocular Effect curve that is similar to the central a(t) curves in the previous modeling. Each eye contributes an excitatory response that is reduced by an inhibitory response from the other eye (bx_1 and (bx_2). A separate binocular fused channel (b_F) combines information from the two eyes in a mechanism that allows for facilitation to take place. The either-eye inhibition (i_L and i_R) act as pre-combination information loss, while the binocular fused channel allows interactions that can act in principle imitate a post-combinatorial information loss such as the central a(t) function. However, this model cannot account for the Experiment 1-3 data.

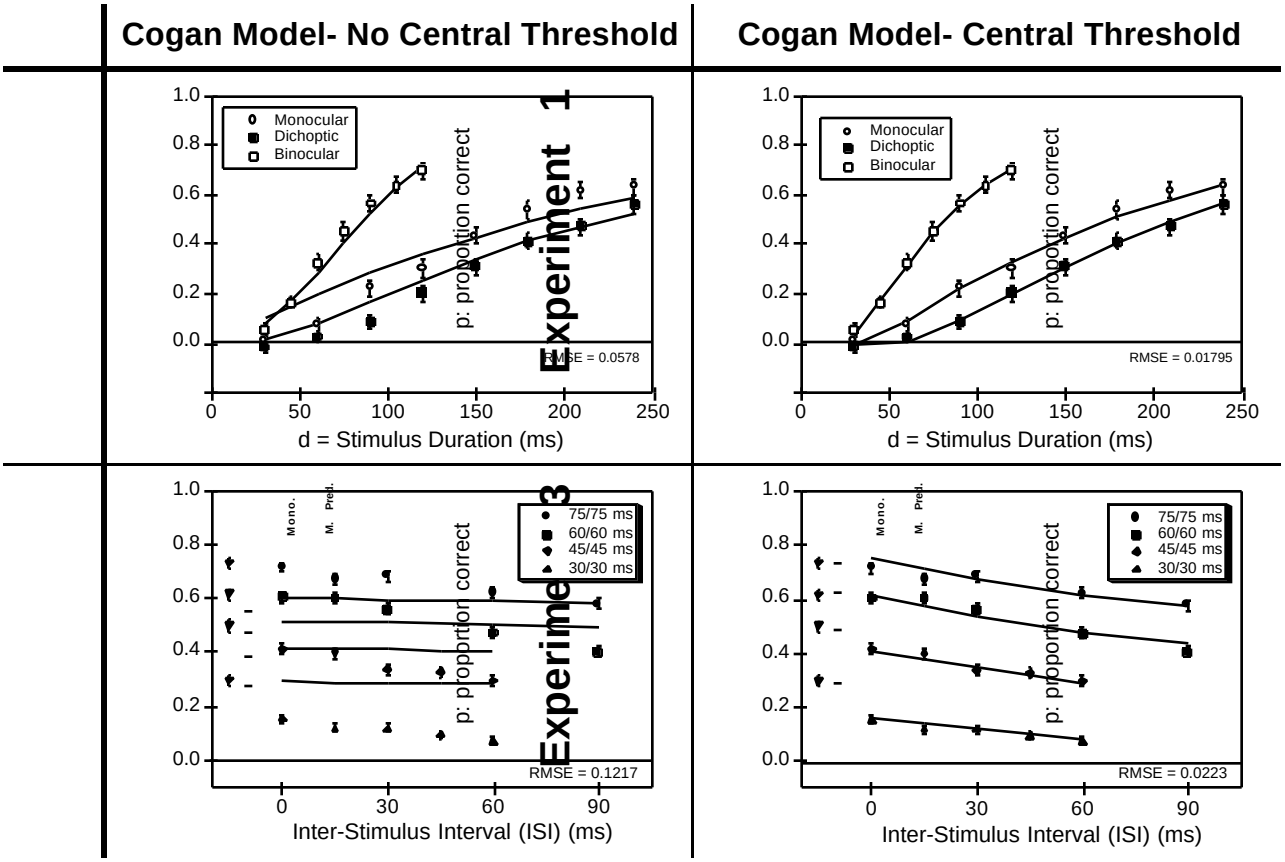

Figure 16. Fits from the Cogan (1987) model to the Experiment 1 and 3 data. Left Panels: The Cogan model cannot completely account for the above-probability summation binocular performance (top left panel) nor the decrease in dichoptic performance with increasing ISI (bottom left panel). Both of these effects require a post-combinatorial source of information loss. Which such an information loss such as a central sensory threshold is added, the revised model gives very good fits at the expense of one more free parameter than the Dual Threshold model.

TABLES

TABLE 1

Luminances And Contrasts For all Experiments. All Luminances are in Candles/m^2. Contrast is Defined as

$$contrast = \frac{L_b - L_f}{L_b + L_f}$$

Where L_b is the Background Luminance, and L_f is the Foreground Luminance.

Experiments 1 and 2

	Digits	Fixation Point
Background	3.502	3.502
Foreground	3.252	1.472
Contrast	0.037	0.408

Experiment 3

	Digits	Fixation Point
Background	8.521	8.521
Foreground	7.392	2.011
Contrast	0.071	0.618

Table 2

Summary of Best-Fitting Linear Summation Model Parameters for Experiments 1-3. Threshold parameters Θ_P and Θ_C are in units of percent contrast, and t and c_S are in units of ms. Note that the RMSE's for Combined Data may not Agree with Figure RMSE's. Table 3 Combined RMSE's are Derived from Parameter Searches on Averaged Data, while Figure RMSE's are computed by comparing averaged model fits and averaged observed Data. The units of RMSE are percent correctly-recalled digits. Note that n =9 for all fits.

Experiment 1: Threshold Model						**Experiment 1: Power Function Model**					
Observer	τ	c_S	Θ_P	Θ_C	RMSE	Observer	τ	c_S	β_P	β_C	RMSE
GW	12.95	4.065	0.463	1.606	0.0333	GW	13.46	0.00869	1.36	2.29	0.03130
TB	7.27	2.373	1.261	1.177	0.0329	TB	7.27	0.000116	2.26	1.92	0.03821
TAK	6.73	2.234	1.316	0.619	0.0367	TAK	5.06	0.000100	3.16	1.35	0.04306
Average	8.02	3.113	0.971	1.103	0.0189	Average	6.13	0.000165	2.54	1.70	0.02056

Experiment 2: Threshold Model						**Experiment 2: Power Function Model**					
Observer	τ	c_S	Θ_P	Θ_C	RMSE	Observer	τ	c_S	β_P	β_C	RMSE
GW	28.55	6.498	0.649	0.159	0.0324	GW	8.39	0.00000150	1.98	2.88	0.02876
TB	24.56	5.154	0.206	0.549	0.0401	TB	13.12	0.0145	1.20	2.35	0.03852
TK	22.39	3.608	0.533	0.370	0.0498	TK	7.99	0.00000465	1.48	3.49	0.04853
GW- No Θ_C	22.16	6.096	1.019	-	0.0318	GW- No β_C	8.74	0.00001292	5.06	-	0.02872

Experiment 3: Linear-summation Model						**Experiment 3: Power Function Model**					
Observer	τ	c_S	Θ_P	Θ_C	RMSE	Observer	τ	c_S	β_P	β_C	RMSE
TB	17.09	3.868	0.143	1.894	0.0482	TB	19.42	0.02846549	1.00967	2.7408	0.0512
LM	15.78	2.245	0.684	0.848	0.0362	LM	2.98	0.00000191	266.209	0.0241	0.0536
MB	14.48	7.565	0.307	1.657	0.0376	MB	10.99	0.09153333	1.16578	2.3177	0.0324
Average	15.33	4.384	0.323	1.414	0.0262	Average	12.22	0.08679971	1.13515	2.1934	0.0387

Note: TAK's Experiment 1 Power Function Model fit was best fit by very small c_S value coupled with a large β_P value. This resulted from trying to fit the . However, when c_S was fixed to a reasonable value (0.0001), the fit was not markedly worse. The best-fitting parameter values were: τ = 2.84, c_S = 1.38E-21, β_P = 12.023, β_C = 1.33, RMSE = 0.04077.

Table 3

Summary of Best-Fitting Cogan Model Parameters for Experiments 1-3. Threshold parameter Θ_C is in units of percent contrast, and t and c_S are in units of ms. Model parameters c and k are from Cogan's 1987 model. Note that n =9 for all fits.

Experiment 1: Original Cogan Model						**Experiment 1: Cogan Model With Central Threshold**						
Observer	τ	c_S	c	k	RMSE	Observer	τ	c_S	c	k	Θ_C	RMSE
GW	4.62	19.51	1.98E-06	33.275	0.0943	GW	14.10	4.769	82.71	52.21	1.840	0.0330
TB	6.66	9.67	1.16E+04	82.276	0.0747	TB	6.47	1.900	48.17	20.82	2.673	0.0327
TAK	31.33	12.77	2.15E+18	433.538	0.0634	TAK	5.66	1.435	32.05	11.36	2.500	0.0370
Average	25.19	9.91	3.44E+06	186.342	0.0563	Average	8.03	3.058	65.13	31.97	2.084	0.0172

Experiment 2: Original Cogan Model						**Experiment 2: Cogan Model With Central Threshold**						
Observer	τ	c_S	c	k	RMSE	Observer	τ	c_S	c	k	Θ_C	RMSE
GW	2.33	17.52	1.39E+05	0.003	0.0946	GW	17.85	5.283	33.6	0.000	1.320	0.0284
TB	0.65	11.71	2.27E+06	0.292	0.1107	TB	23.13	5.036	73.7	57.52	0.808	0.0413
TK	1.60	9.62	2.48E+05	0.004	0.1384	TK	22.22	3.314	34.4	3.585	0.958	0.0469

Experiment 3: Original Cogan Model						**Experiment 3: Cogan Model With Central Threshold**						
Observer	τ	c_S	c	k	RMSE	Observer	τ	c_S	c	k	Θ_C	RMSE
TB	28.12	15.72	5.36E-03	49.72	0.1403	TB	30.00	6.361	4383	152.3	0.687	0.0330
LM	58.84	5.02	4.24E+11	250.4	0.0786	LM	27.08	2.708	649.5	118.4	0.779	0.0297
MB	0.80	21.75	9.41E-06	78.97	0.0953	MB	14.10	6.892	5.497	0.000	2.153	0.0376
Average	31.06	12.95	2.46E-04	19.95	0.1221	Average	20.96	5.629	446.1	97.78	0.891	0.0202

Note: All model fits were substantially worse than the corresponding Dual-Threshold fits of Table 2. As a result of this lack of fit, the best-fitting parameter values are often extreme values as the model is stressed to accommodate the data. When a central non-linearity is added, the values for c and k exhibit much more regularity.